Characterization of posttranscriptional regulation elements – From protein degradation to functional RNA structures

PhD Thesis

TECHNISCHE UNIVERSITÄT DARMSTADT

Vom Fachbereich Biologie der

Technischen Universität Darmstadt

Zur Erlangung des akademischen Grades eines

Doctor rerum naturalium

(Dr. rer. nat.)

genehmigte Dissertation von

Herr M. Sc. Stephen Peter

Erstgutachterin: PD Dr. Julia Weigand

Zweitgutachterin: Prof. Dr. Beatrix Süß

Darmstadt 2022

Peter, Stephen: Characterization of posttranscriptional regulation elements – From protein degradation to functional RNA structures

Darmstadt, Technische Universität Darmstadt,
Jahr der Veröffentlichung der Dissertation auf TUprints: 2022
URN: urn:nbn:de:tuda-tuprints-211953
Tag der mündlichen Prüfung: 25.03.2022

1. Index

2. Abstract

Posttranscriptional gene regulation in eukaryotic cells is one of the most important mechanism in complex life to either control protein synthesis or diversity at any given moment in the life of a cell. Consequently, deregulation of the many processes involved in posttranscriptional regulation can lead to severe diseases, such as Alzheimer's disease or certain types of cancer.

RNA-binding proteins (RBPs) can also facilitate alternative splicing (AS), which increases protein diversity and fine tunes the protein amount and function in the case of different stress conditions. A deregulation of AS events can lead to severe diseases, such as Parkinson's disease or certain cancer variants. I characterized a newly described mechanism, where AS events are coupled to rapid protein decay. We termed this event AS-CPD, alternative splicing coupled to constitutive protein decay. The protein decay signal (degron) found in mammalian cells is also functional in *Saccharomyces* (*S.*) *cerevisiae* and *Escherichia* (*E.*) *coli* cells. It is dependent on hydrophobic amino acids in the C-terminus and has the capability to rapidly and efficiently reduce the amount of the tagged protein to an undetectable amount in mere minutes. This mechanism might be due to a conserved stress response in the tested organism. The degron described in this thesis could be a potential tool for new kinetic analysis.

Major players in posttranscriptional regulation are *trans*-acting RBPs, such as Roquin or AUF1. Roquin is a key regulator in immune homeostasis and recognises stem-loop (SL) structures in 3'-UTRs (untranslated regions) to destabilise certain messenger RNAs (mRNAs). In this study, we found, that Roquin can recognise not only classical constitutive decay elements (CDEs), but also AU-rich decay element (ARE)-like CDEs. The binding of these elements may also be subject to competition between different RBPs, as it is in the case of the *UCP3* 3'-UTR CDEs. Here, Roquin and AUF1 compete for the binding to CDE1.

RNA structure often implies a certain function in the organism. The pandemic causing virus SARS-CoV-2 is an RNA virus with a 30 kb long heavily structured genome. The many SLs in the 5'- and 3'-UTRs fulfil different essential functions, which are partially unknown. Here, we provide a detailed analysis of the structure of the genome and impose a screen of chemical compounds with the ability to bind RNA. We found a potent binder D01 with the ability to bind the pseudoknot in between the two open reading frames (ORFs) 1a and 1b, which encode different and essential parts of the viral proteome. These compounds might be a precursor for future potent drugs, able to target RNA viruses with structured genomes.

3. Zusammenfassung

Posttranskriptionelle Genregulation in eukaryotischen Zellen ist einer der bedeutendsten Mechanismen in komplexen Lebewesen, um einerseits die Proteinsynthese oder die Protein-Diversität zu jedem Zeitpunkt beeinflussen zu können. Eine Deregulation der vielen Prozesse, die posttranskriptionelle Regulation beinhalten, können zu schweren Krankheiten, wie zum Beispiel Alzheimer oder verschiedenen Krebsarten führen.

RNA-bindende Proteine (RBPs) sind am alternativen Spleißen beteiligt, wodurch die Protein-Diversität erhöht wird. Dies wiederum dient zur Feinjustierung der Proteinmenge oder -Funktion bei verschiedenen Arten von Stress. Eine Deregulation von AS kann zu verschiedenen Krankheitsbildern, wie zum Beispiel Parkinson oder verschiedenen Krebsarten führen. Ich konnte einen neuen Mechanismus beschreiben, der alternatives Spleißen mit rapiden Proteinabbau in Verbindung bringt. Diesen Mechanismus haben wir AS-CPD genannt, *alternative splicing coupled to constitutive protein decay*. Das Proteindegradationssignal (Degron), dass wir in menschlichen Zellen gefunden haben, ist auch in *Saccharomyces* (S.) cerevisiae und *Escherichia* (*E.*) *coli* Zellen funktional. Es ist von hydrophoben Aminosäuren im C-Terminus abhängig und hat die Fähigkeit schnell und effizient die Zielproteine in wenigen Minuten zu degradieren. Diesem Mechanismus könnte eine konservierte Stressantwort zu Grunde liegen. Das von mir beschriebene Degron könnte ein potentielles Werkzeug für Enzymkinetik-Untersuchungen darstellen.

Wichtige Faktoren der posttranskriptionellen Regulation sind *trans*-agierende RBPs, wie beispielsweise Roquin oder AUF1. Roquin ist ein wichtiger Faktor in der Immunhomöostase und erkennt Stammschleifenstrukturen im 3'-untranslatiertem Bereich (UTR) um bestimmte mRNAs zu destabilisieren. Wir fanden heraus, dass Roquin nicht nur klassische *constitutive decay elements* (CDEs), sondern auch AU-reiche *decay elements* (ARE)-ähnliche CDEs erkennt. Die Bindung dieser Elemente unterliegt einer Konkurrenz verschiedener RBPs, so wie es bei dem 3'-UTR von *UCP3* der Fall ist. In unserem beschriebenen Fall, konkurrieren AUF1 und Roquin um die Bindung an CDE1.

RNA Strukturen haben oft eine Funktion in einem Organismus. Das pandemische Virus SARS-CoV-2 hat ein ca. 30 kb langes, stark strukturiertes Genom. Die vielen Stammschleifen im 5'- und 3'-UTR haben unterschiedliche, essentielle Funktionen, die zum Teil unbekannt sind. In unseren Studien zeigen wir detaillierte Strukturen des Genoms und stellen einen Screen kleiner chemischer Komponenten, die eine RNA Bindefähigkeit haben, vor. Wir haben einen potenten Binder D01 gefunden, der den Pseudoknoten zwischen den offenen Leserahmen 1a und 1b bindet. Diese Leserahmen codieren essentielle Proteine des Virus Genoms. Der Binder D01 könnte ein Vorläufer Medikament gegen RNA Viren mit strukturiertem Genom sein.

4. Introduction

Posttranscriptional gene regulation in eukaryotic cells is a complex and tightly controlled mechanism, which is commonly described as a process to direct protein synthesis via the genetic code. The regulation of a messenger RNA (mRNA) is achieved at all stages of its "life", starting with the transcription, pre-mRNA splicing, mRNA export, translation and finally its decay. All these mechanisms are controlled by RNA-binding proteins (RBPs). These RBPs, can for example, bind the 3'-untranslated region (UTR) of an mRNA and vary the stability of respective mRNA, resulting in reduced or increased protein abundance. Protein abundance is not only controlled at RNA level, but also post-translationally at protein level, e.g. by posttranslational modifications (PTMs) or by degrons. A degron is an N- or C-terminal amino acid sequence, which marks a protein for degradation. Protein decay is mostly carried out by the 20S or 26S proteasome in mammalian cells.

This doctoral thesis focuses on the understanding of a novel mechanism of how alternative splicing controls protein abundance as well as the importance of RNA structures in posttranscriptional gene regulation and for viral replication.

4.1. Pre-mRNA splicing

In eukaryotic cells, protein-coding mRNAs are transcribed from genes as pre-mRNAs in the nucleus and then undergo several processing steps, e.g. 5'-capping, pre-mRNA splicing and 3'-end processing. These processes are tightly regulated and coordinated with each other to achieve accurate and efficient gene expression (Carey and Wickramasinghe, 2018; Rambout et al., 2018). After processing the mature mRNA is exported into the cytoplasm for translation.

A pre-mRNA contains exonic and intronic sequences. The introns have to be removed by splicing, prior to export into the cytoplasm. Splicing is carried out by the spliceosome, a massive structure, in which five small nuclear ribonucleoprotein particles (snRNPs) and a large number of auxiliary proteins cooperate to accurately recognize the splice sites (SS) and catalyse the two steps of the splicing reaction. These two reaction steps consist of transesterification steps, each involving a nucleophilic attack on terminal phosphodiester bonds of the intron. The spliceosome recognises the sequence GURAGU, which indicates the 5'-SS within the introns. The 3'-SS contains a polypyrimidine tract and a terminal YAG motif. Introns also contain a branch point sequence with an invariant adenosine 18-40 nucleotides (nts) upstream of the 3'-SS. In the first step, the reaction is carried out by the 2'-hydroxyl (2'-OH) of the branch point adenosine and in the second step by the 3'-OH of the last nucleotide of the upstream exon. The 5'-end of the intron is ligated with the branch point adenosine

through a nucleophilic attack of the 2'-OH on the 5'-SS. In a second step the free 3'-OH of the 5'-SS reacts with the phosphate of the 3'-SS, whereby the exons are connected and the intron is removed (**Figure 3.1.1**) (Chen and Manley, 2009; Cieply and Carstens, 2015; De Conti et al., 2013).

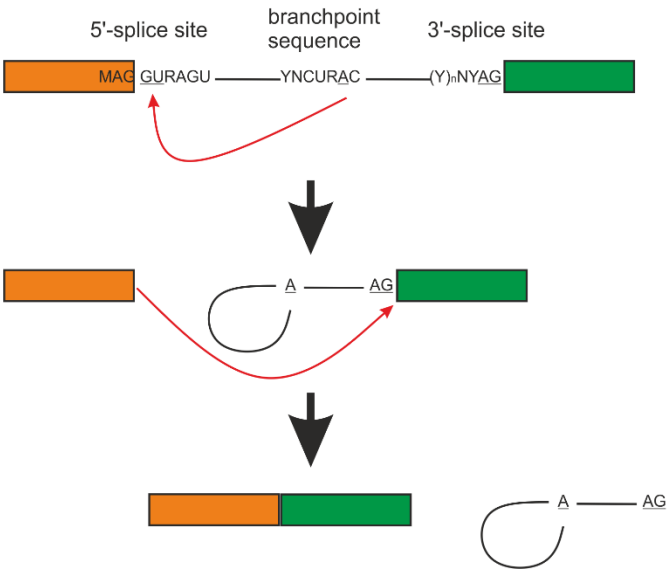

Figure 3.1.1: The splicing reaction is carried out in two subsequent transesterifications as described in the text.

Essential components of the U2-dependent spliceosome are the five small nuclear ribonucleoproteins (snRNPs): U1, U2, U4, U5 and U6. Each snRNP contains a uridine-rich snRNA, a set of seven (L)Sm proteins and numerous snRNP specific proteins (Deckert et al., 2006; Wahl et al., 2009). Splicing is a highly dynamic process, which leads to several new conformations of the spliceosome during the whole splicing process, which often includes many different factors. If the spliced intron does not exceed 200-250 nt, the spliceosome is directly constituted across the intron. However, the introns of higher eukaryotes most often exceed 250 nt. Thus, the spliceosome is first assembled across an exon. These processes are called intron or exon definition (Cieply and Carstens, 2015; Fox-Walsh et al., 2005). During intron definition the U1 snRNP is recruited to the 5'-SS. The splicing factors SF1/mBBP and U2 auxiliary factor (U2AF) recognize the branch site, the polypyrimidine tract and the 3'-SS. This process is ATP dependent and results in the building of complex E. The next ATP-dependent step is binding of the U2 snRNP to the branch point, building complex A. Further recruitment of the U4/U6-U5 tri-snRNP complex leads to the formation of the B complex, which is converted into the catalytically active C complex after extensive conformational changes and remodelling (Chen and Manley, 2009; Cieply and Carstens, 2015). The following RNA-RNA as well as RNA-protein interactions lead to destabilization of the U1 and U4 snRNPs and to the

activation of the spliceosome catalysing the first splicing step. Then complex C is assembled, which completes the splicing process by executing the second catalysis step. The spliceosome is disassembled and the involved snRNPs are reused for further splicing processes (Wahl et al., 2009; Will and Lührmann, 2011) (Figure 3.1.2). During exon definition, the U1 snRNP binds downstream of the exon and recruits U2AF to the upstream polypyrimidine tract of the 3'-SS. The U2 snRNP binds to the branch point upstream of the exon. The complex is stabilised by SR (serine-arginine)-rich proteins, which can bind exonic splicing enhancer (ESE) elements within the exon. The complex then shifts subsequently from the exon definition to the cross-intron complex. This process however is not fully understood (Wahl et al., 2009; Will and Lührmann, 2011).

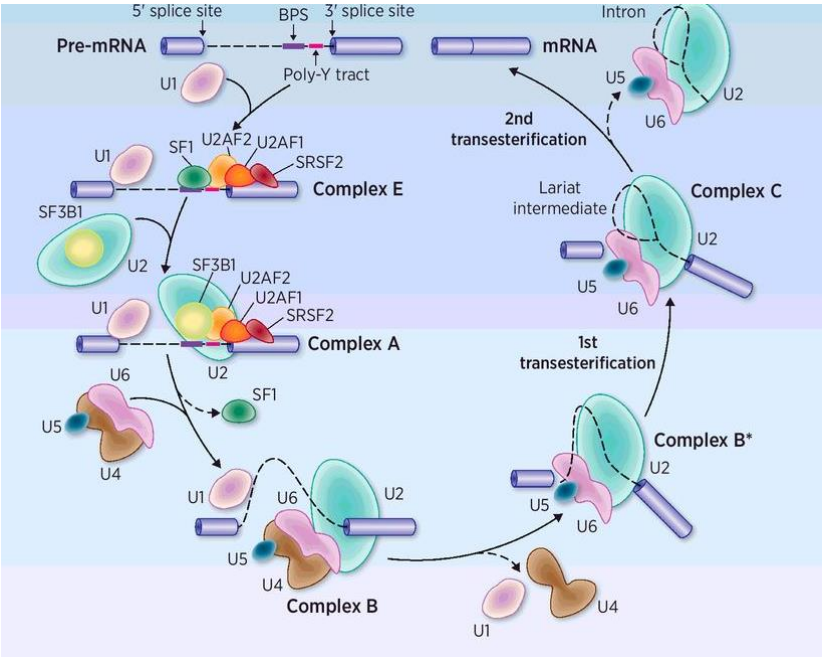

Figure 3.1.2: Pre-mRNA splicing by the U2 spliceosome. The exact mechanism depicted is described in the text above. In short: the 5'-SS is recognized by the U1 snRNP, which in turn recruits SF1 and U2AF1/2/SRSF2 building complex E. Complex E is then transformed into complex A by binding of the U2 snRNP. After release of SF1 and recruitment of the U4/6-5 tri-snRNP the intron is removed. The various spliceosomal complexes are named according to metazoan nomenclature. Exon and intron sequences are indicated by the boxes and lines. Modified after https://clincancerres.aacrjournals.org/content/clincanres/23/2/336/F1.large.jpg (29.06.2021, 4:08 pm).

4.2. Alternative splicing

The human transcriptome is more diverse than the genes encoded by the genome. This results from different isoforms arising out of the pre-mRNA in a process called alternative splicing (Kim

et al., 2018). Alternative splicing (AS) is an essential process that allows for considerable proteomic diversity and complexity despite a relative limited number of genes (Graveley, 2001). About 95% of human multi-exonic genes are alternatively spliced, to give rise to different protein isoforms that can vary with respect to protein-protein interaction, stimulatory or inhibitory activities or subcellular location (Graveley, 2001). AS is important for tissue-specific gene expression and enables distinct gene expression in different cell types (Wang et al., 2008). General disruption of the splicing machinery causes the death of an organism. Even modest alterations in AS can produce malfunctioning proteins, which can result in organ dysfunction and various disease states (Kim et al., 2018; Tazi et al., 2009). AS can fail by mutation of splicing signals or also by mutation of splicing factors, such as heterogenous nuclear ribonucleoproteins (hnRNPs) or SR proteins, promoting different pathologies, e.g. cancer development (Scotti and Swanson, 2016; Sterne-Weiler and Sanford, 2014). AS can be activated by spontaneous stimuli from the environment, such as hypoxia or reactive oxygen species (ROS). AS can act as a switch, activating regulatory pathways and therefore possibly sustain survival of the cell (Kelemen et al., 2013). Interestingly, AS can lead to significant differences in protein function in order to cope with a changing environment (Gallego-Paez et al., 2017).

AS mainly occurs in five different types: cassette exons, mutually exclusive exons, alternative 5'-SS, alternative 3'-SS and intron retention (**Figure 3.2.1**). The most common AS event in mammals involves cassette exons. A cassette exon might be included in or excluded from the mature mRNA. In some cases two neighbouring cassette exons can be mutually exclusive (MXE), which is a rare case in mammals. Here, either the first or the second exon can be included in the mature mRNA. Further alternative splicing events are the use of alternative 5'- or 3'-SS, leading to longer or shorter exons. In some cases an intron can be retained, to create a new mature mRNA (McManus and Graveley, 2011; Pohl et al., 2013).

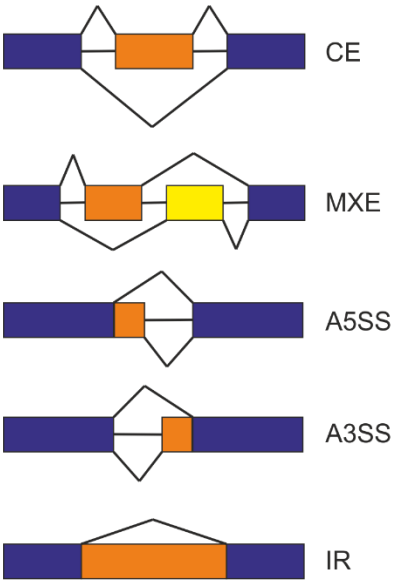

Figure 3.2.1: Different types of AS. CE = cassette exon, MXE = mutually exclusive exon, A5SS = alternative 5'-SS, A3SS = alternative 3'-SS, IR= intron retention. Constitutive exons are shown in blue. Alternative included parts in orange/yellow.

Precise regulation of AS, which is important for mRNA maturation and hence protein synthesis, requires many factors facilitating the accurate selection of splice sites and the subsequent splicing process (Tazi et al., 2009). The splicing decision is mediated by splicing factors. These factors include the core spliceosome, SR proteins and hnRNPs, which bind to splicing regulatory elements (SREs). Exon recognition and selection of splice sites are regulated by *trans*-acting repressors and activators and corresponding *cis*-acting silencer and enhancer elements on the pre-mRNA. The decision as to which frequency an exon is included in the mature mRNA, involves protein regulators and RNA sequence elements. These elements can vary in function and position, giving rise to four categories: intronic splicing enhancer (ISE), intronic splicing silencer (ISS) or exonic splicing enhancer (ESE) and exonic splicing silencer (ESS). ESEs are usually bound by members of the SR protein family (Graveley, 2000; Long and Caceres, 2009). The SR proteins recognize ESEs by their RNA recognition motifs (RRM) and mediate protein-protein interactions and perhaps protein-RNA interactions with their Arginine-Serine repeat-containing domains (RS domains). These SR proteins enhance transcription, while binding an ESE in the exon. Binding in the intronic sequence causes a silencing of the splicing event. ESS are commonly bound by hnRNPs, which have one or more RNA-binding domains and protein-protein interaction domains (Chen and Manley, 2009; Cieply and Carstens, 2015; Glisovic et al., 2008). These hnRNPs assist in maturing of newly formed pre-mRNAs into mRNA, stabilize the mRNA during cellular transport and control its translation (Geuens et al., 2016).

4.2.1. Unproductive splicing

AS is used by the cell not only to increase proteome diversity, but also to rapidly adapt to a changing environment (Farina et al., 2020; Filichkin et al., 2015; Pagliarini et al., 2015; Ule and Blencowe, 2019). For example, changes in exon inclusion rates allow for the fine-tuned production of proteins with different enzymatic activities, cellular localization and protein-protein-interactions. Apart from the generation of protein isoforms, AS is used for quantitative changes of protein levels by unproductive splicing, i.e. by deliberate production of non-coding mRNA isoforms. The best studied mechanism in this regard is AS coupled to the nonsense-mediated decay (NMD) pathway (Dyle et al., 2020; Kurosaki et al., 2019). NMD is a translation-dependent mRNA quality control pathway that selectively degrades mRNAs harbouring a premature termination codon (PTC), i.e. a stop-codon 50-55 nts upstream of an exon-exon junction (**Figure 3.2.1.1**). PTCs can be introduced into the mRNA by mutations during transcription or by errors during mRNA processing causing a change in the codon, which could in turn create a stop codon (Arribere and Fire, n.d.; Kurosaki et al., 2019).

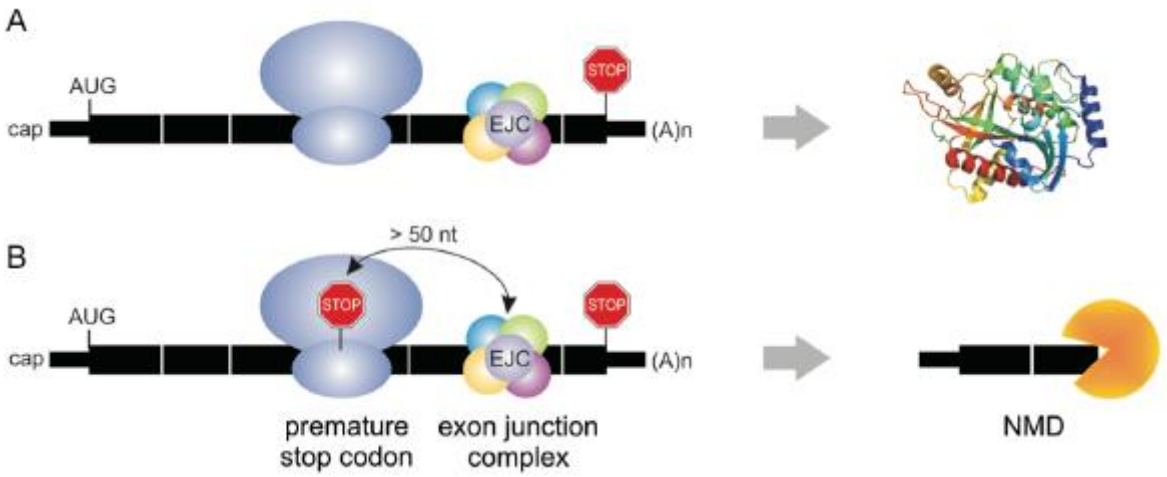

Figure 3.2.1.1: **Scheme of nonsense-mediated decay**. (A) Normal translation of the mRNA with a stop-codon at the end of the open reading frame (ORF). (B) A premature termination codon (PTC; STOP in figure) causes a degradation of the mRNA through NMD.

AS events creating a premature stop codon lower overall protein levels by production of non-coding mRNA variants and thus concomitant reduction in mRNAs coding for full-length proteins. If a premature stop codon is created during an AS event, the exon containing the premature stop codon, is called poison exon. AS-NMD is regarded as a widespread regulation mechanism, which ensures protein homeostasis, e.g. by autoregulation of RNA-binding proteins (RBPs) (Fischer et al., 2020; Kemmerer et al., 2018; Müller-McNicoll et al., 2019). Today it is known, that 40% of all human genes are regulated via AS-NMD (Chang et al., 2007;

Lewis et al., 2003). One such example of AS-NMD occurs in the Myc-associated factor X (MAX) under hypoxia (see chapter 3.4.3) (Kemmerer and Weigand, 2014).

4.3. Hypoxia

Hypoxia, in general, is the state of insufficient oxygen supply. Although oxygen is essential for cell viability, hypoxic signalling plays an important role in many physiological processes. It is implicated in embryonic development, wound healing or occurs at high altitudes (Dunwoodie, 2009; Li et al., 2007; Simonson et al., 2010). There are five types of tissue hypoxia. Hypoxemia is marked by a reduced partial oxygen blood pressure, which is caused by high altitude. Anemic hypoxia is caused by a reduced level of haemoglobin in the blood, mostly resulting from iron deficiency. Ischemic hypoxia results from a reduced blood circulation. Diffusional hypoxia occurs, as the name suggests, when diffusion distances are increased. The cell can also lose the ability to use oxygen by intoxication e.g. with cyanides. This loss of ability is then called cytotoxic hypoxia (Choudhury, 2018; Höckel and Vaupel, 2001).

An important means of counteracting hypoxia is the distribution of blood vessels, which provide the surrounding tissue with oxygen and metabolites. The inner lining of blood vessels consists of endothelial cells, which are thus the first cells to be affected by hypoxemic, anemic or ischemic hypoxia (Choudhury, 2018; Fraisl et al., 2009; Potente et al., 2011). Hypoxia changes the gene expression of endothelial cells extensively. It promotes gene expression programs, which lead to increased proliferation, migration and angiogenesis (Choudhury, 2018; Fraisl et al., 2009). Hypoxia affects tumour cells in the very same way, as it affects the endothelial cells. It likewise induces gene expression programs, increasing proliferation and energy uptake (Choudhury, 2018; Muz et al., 2015).

4.3.1. Transcriptional regulation under hypoxia

The protein family generally orchestrating transcription changes under hypoxia is the family of hypoxia inducible factors (HIFs) (Carroll and Ashcroft, 2005; Schito and Semenza, 2016; Semenza, 2017). The discovery of the mechanism and the HIF protein family was awarded with the Nobel Prize in Physiology or Medicine 2019. The HIF complex consists of two subunits, HIF-α and -β. The α-subunit can be differentiated into 3 subtypes: HIF-1α, HIF-2α (also known as EPAS1) and HIF-3α (Chee et al., 2019; Schito and Semenza, 2016). HIF-1α is constitutively synthetized and present in the cytosol (Schito and Semenza, 2016; Semenza, 2017). Under normoxic conditions HIF1-α is hydroxylated at conserved proline residues by prolyl hydroxylases (PHD1-3). The hydroxylated protein is then marked by the von Hippel-Lindau tumour suppressor protein (VHL protein) for degradation by the proteasome. Under hypoxic conditions, these prolyl hydroxylases are inhibited, HIF-1α is stabilized and can form a heterodimer with HIF-1β (also aryl hydrocarbon receptor nuclear translator; ARNT). The

dimer diffuses into the nucleus and binds to hypoxia responsive elements (HREs; **Figure 3.3.1.1**) to activate transcription of genes involved in glycolysis, cell proliferation, angiogenesis and erythropoiesis (Lee et al., 2019; Meijer et al., 2012).

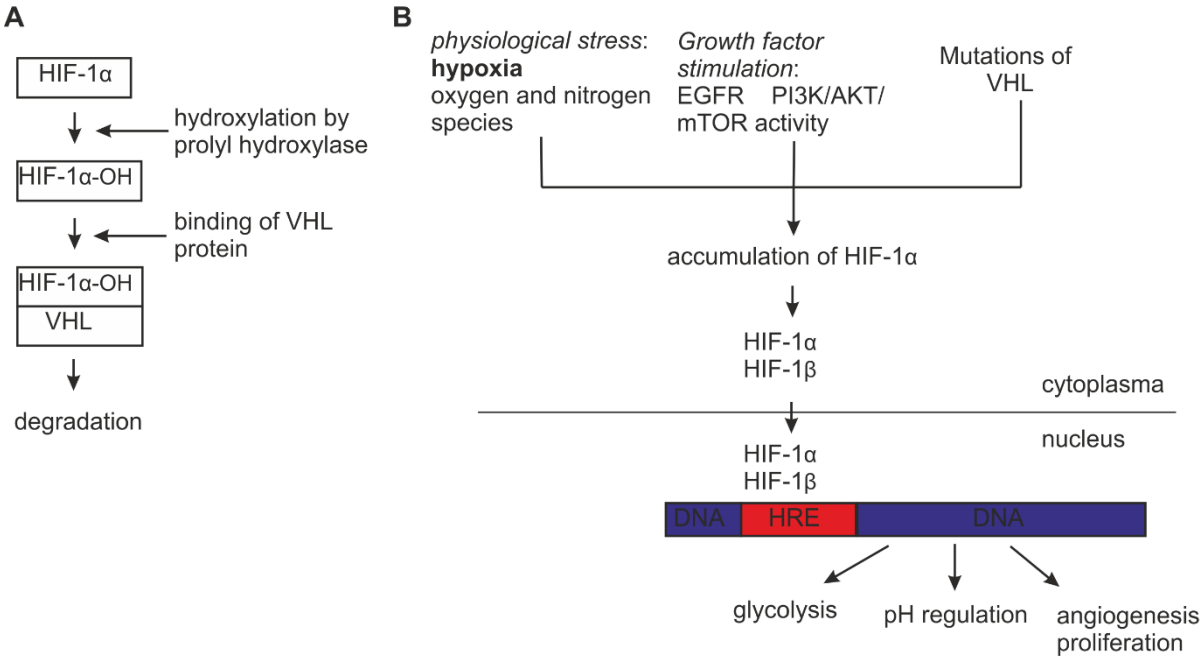

Figure 3.3.1.1: HIF transcriptional regulation pathway. (A) Under normoxia HIF-1α is hydroxylated and degraded. (B) Under hypoxia HIF-1α accumulates and dimerizes with HIF-1β. Growth factor stimulation or mutations of the VHL protein can also lead to HIF-1α accumulation. The HIF complex activates the transcription of target genes implicated in glycolysis, pH regulation, angiogenesis and proliferation.

Some examples for induced genes are lactate dehydrogenase *(LDHA)*, erythropoietin *(EPO)* or vascular endothelial growth factor A *(VEGFA)* (Cui et al., 2017; Haase, 2013; Lee et al., 2019). The two other HIF-α proteins (HIF-2α and HIF-3α) are also induced during hypoxia as described for HIF-1α. While a splice variant of HIF-3α (HIF-3α4) is important for an acute hypoxia response and forms an abortive complex with HIF-2α, HIF-2α is accumulated later and important for prolonged hypoxic gene activation (Holmquist-Mengelbier et al., 2006; Maynard et al., 2007; Tanaka et al., 2009). The role of HIF-3α in hypoxia adaptation is still under discussion, as it seems to inhibit the activities of HIF-1 and HIF-2 complexes (Makino et al., 2001). In other cases, such as during pancreatic cancer, HIF-3α promotes metastasis (Zhou et al., 2018).

4.4. MAX

On top of the transcriptional changes, hypoxia likewise induces a multitude of changes in posttranscriptional gene regulation, e.g. alternative splicing events (Fischer et al., 2020; Weigand et al., 2012). One example of changed alternative splicing during hypoxic stress is the mRNA of the protein MAX (Myc-associated factor X) (Kemmerer and Weigand, 2014). The protein belongs to the basic-helix-loop-helix-leucine-zipper (bHLHLZ) protein family. The mRNA encoding the MAX wild type protein consists of 4-5 exons (**Figure 3.4.3.1**) (Blackwood et al., 1992; Diolaiti et al., 2015; Kemmerer and Weigand, 2014; Nair and Burley, 2003). The translated protein contains a basic region, for DNA binding, and a helix-loop-helix-leucine-zipper region. The latter is necessary for dimerization with other bHLHLZ proteins (Cascón and Robledo, 2012; Sammak et al., 2019; Sicoli et al., 2019).

4.4.1. MAX transcription network

MAX is a ubiquitously expressed transcription factor and the central factor in a network of transcription factors (Diolaiti et al., 2015). MAX is participating in the regulation of apoptosis, differentiation, proliferation and transformation. MAX can form heterodimers with other bHLHLZ proteins such as MYC or MXD. The effect on transcription is depending on the binding partner (**Figure 3.4.1.1**). The most prominent binding partner of MAX is the oncogene MYC. The protein MYC consist of a bHLHLZ-domain at the C-terminus and a transcriptional activation domain (TAD) located near the N-terminus. Within the TAD, MYC family members contain two conserved domains termed MYC Box I and MYC Box II. These boxes are necessary for MYC protein stability (MYC Box I) and for interaction with components of histone acetyltransferases (MYC Box II) (McMahon et al., 2000, 1998). Since the MAX protein is lacking any other interaction domain than the bHLHLZ domain, it is considered to only mediate the binding of different interaction partners to DNA (Ayer et al., 1993; Diolaiti et al., 2015). However, MAX protein can also efficiently form homodimers, which are speculated to inhibit transcription by silent DNA binding (Cascón and Robledo, 2012; Castell et al., 2018; Diolaiti et al., 2015; Grandori et al., 2000). MXD proteins efficiently compete with MYC for the heterodimeric binding of MAX *in vitro* (Ayer et al., 1993). The different MAX complexes than compete for binding the same E-Box containing DNA consensus sequence (CACGTG or CANNTG) in the promotor region of many different genes, regulating gene expression. While MAX/MYC complexes recruit proteins, which change repressive to active histone modification and increase transcription elongation, MAX/MXD complexes do the opposite (Allevato et al., 2017; Diolaiti et al., 2015). They function as transcriptional repressors (MAX-MXD1) or are unable to activate transcription (MAX-MXD2) (Ayer et al., 1993; Zervos et al., 1993).

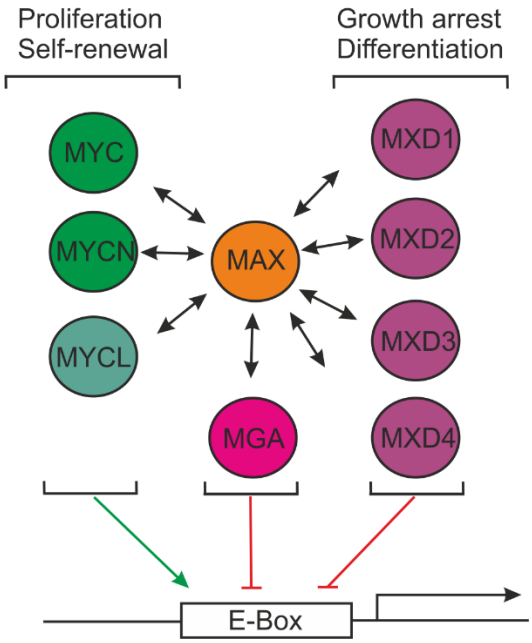

Figure 3.4.1.1: Diagram of the MAX network. The green arrow pointing to the E-Box indicates activation of transcription, while the red lines indicate inhibition.

MAX protein levels are mainly unchanged during the cell cycle and the *MAX* gene is expressed broadly during development. The MAX wild type protein is very stable with an half-life of > 24 h and there are little known posttranscriptional regulations (Blackwood et al., 1992). Two miRNAs (miR-22 and miR-193b) are known to reduce *MAX* gene expression and thus inhibit cell cycle progression in normal and tumour cells (Berenguer et al., 2013; Ting et al., 2010). *MYC* expression, in contrast, is highly regulated. MYC protein levels are high during the proliferating cell cycle and peak at the entry of G0 to G1 transition (Rabbitts et al., 1985). High levels of MYC inhibit differentiation of many cells and induce reprogramming to induced pluripotent stem cells (Leon et al., 2009; Takahashi and Yamanaka, 2006). An example for decreasing MYC level during differentiation are hematopoietic cells. During differentiation MYC protein levels decrease, while MXD1 protein levels increase (Ayer and Eisenman, 1993; Hurlin et al., 1994; Larsson et al., 1997). Since the MXD1 and MXD2 proteins have contrary functions to MYC, their expression peaks during differentiation and cell cycle exit (Quéva et al., 1998). The contrasting effect of MYC and MXD is highlighted by the following experiment: a chimeric protein containing the MYC bHLHLZ domain fused to the MXD1 transcriptional repression domain repressed MYC target genes and efficiently induced differentiation in the erythro-leukemia cell line K562 (Acosta et al., 2008).

Interestingly, *Max* null murine embryonic stem cells expressing an inducible *Max* gene cease proliferating, start to differentiate and eventually undergo apoptosis, when *Max* expression is not induced (Hishida et al., 2011). Likewise, deletion of *MAX* in premalignant Eμ-*Myc* cells

causes an arrest in lymphomagenesis. In addition, the deletion causes a global down-regulation of *Myc*-activated genes, a significant reduction of MYC protein level and a reduction in transcriptional targets, that increase MYC stability (Mathsyaraja et al., 2019). These experiments underline the central importance of MAX for the function of the transcriptional network.

4.4.2. MAX in disease

Dysregulation of the MYC/MAX/MXD network is often found in cancer. Best studied in this context is *MYC* overexpression. Since MYC is part of a greater network, the deregulation of one member has a strong impact on the whole network. This theory is based on the facts, that certain members, such as MYC or MXD compete for binding to MAX. The alteration of the heterodimer then can bind similar or related DNA sequences and thus have a strong impact on transcription and the organism as whole. Unfortunately, while much is known about MYC as a driving factor of oncogenesis and tumour growth, little is known about the role of MAX alone.

Recently, it was shown that MAX plays an important role in anaplastic large cell lymphoma (ALCL) and peripheral T-cell lymphoma (PTCL-NOS). ALCL patients lacking the *MAX* gene expression had an inferior prognosis compared to patients with *MAX* expression. Moreover, immunohistology analysis revealed, that patients without MAX display different morphological variants, e.g. predominantly small cell- or neutrophil-rich variants, which are known to be more aggressive in proliferation (Yamashita et al., 2020). Accordingly, it was suggested to use MAX as a biomarker for poor prognosis and cancer development. Moreover, in some cancer types, such as non-small cell lung cancer or neuroendocrine tumours, *MAX* is homozygously mutated, causing the complete loss of MAX protein (Berberich and Cole, 1992; Romero et al., 2014).

4.4.3. Alternative splicing of MAX

The MAX protein consists of 4-5 exons (see **Figure 3.4.3.1)**. The two wild type proteins, which can include or exclude exon 2, has 160 or 153 amino acids, respectively. Under hypoxia two additional isoforms are induced by AS, isoform C and isoform E (Kemmerer and Weigand, 2014). Isoform C contains a poison exon and is therefore subject to NMD. In isoform E the intron between exon 4 and 5 is retained, creating a variant with an alternative C-terminus. This alternative C-terminus contains a degron, which causes rapid protein degradation.

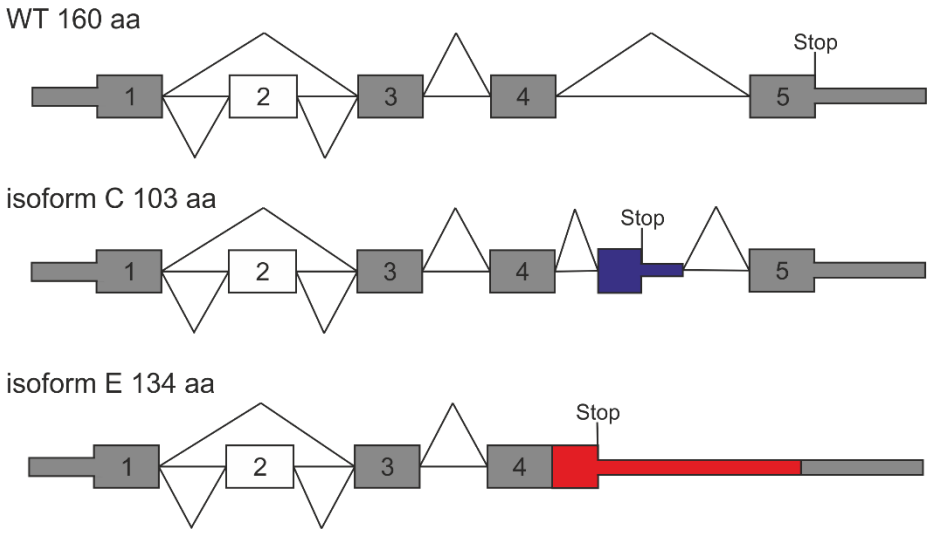

Figure 3.4.3.1: Exon scheme of *MAX* pre-mRNA isoforms. The numbers indicate the exons. The lines indicate a splicing event, while "Stop" indicates a termination codon. The second exon is a cassette exon. aa = amino acids.

There are only few posttranscriptional regulations known for *MAX* expression. Strikingly, Kemmerer and Weigand could identify a novel posttranscriptional regulation under hypoxia. Under hypoxia, *MAX* is alternatively spliced to create two isoforms, isoform C and E (Kemmerer and Weigand, 2014). Isoform C includes a poison exon, which triggers NMD (see figure **3.4.3.1**). In isoform E, the last intron is retained, which leads to a C-terminally truncated protein variant, which contains 36 alternative, isoform-specific amino acids (aa). This isoform escapes AS-NMD, as the stop-codon resides within the last exon, i.e. it is not located upstream of an exon-junction complex (Kemmerer and Weigand, 2014). Still, this splicing event is unproductive, by producing an mRNA encoding an extremely unstable MAX protein variant. Thus, the hypoxia-induced alternative splicing of *MAX* pre-mRNA creates alternative isoforms, which both lead to non-functional proteins. The two isoforms are considered to reduce the amount of wild type protein, which will in turn, reduce the amount of MAX able to form heterodimers (Diolaiti et al., 2015; Kemmerer and Weigand, 2014).

Why the encoded MAX protein variant is unstable was unclear. I could identify that the isoform specific amino acids create an extremely efficient degradation tag, which I termed isoE C-degron. This degron marks the protein for rapid decay (Peter et al., 2021).

4.5. Protein degradation

Targeted protein degradation serves to tightly regulate protein levels in response to internal or external signals, such as hypoxia or stress. It is also a mechanism to protect the cell from misfolded, aggregated and otherwise abnormal proteins (Davies, 2001; Kopito, 2000;

Varshavsky, 2019). These proteins have to be degraded fast, to avoid inclusion bodies, which further increase the stress of the cell. Defects in protein degradation, such as mutations or inhibitions, can cause diseases, e.g. Alzheimer's disease (McKinnon and Tabrizi, 2014). The following chapter will focus on the proteasome and the ubiquitin degradation pathway.

4.5.1. The proteasome

The gross amount of protein degradation in mammals is mediated by the 26S proteasome, a multi-catalytic ATP-dependent protease complex, which contains a so-called AAA ATPase. These ATPases convert the energy of ATP hydrolysis into mechanical force though conformational changes in their subunits to cope with unfolding of substrate proteins and synergistically act with proteases. The proteasome is a multi-subunit complex consisting of a 19S regulatory particle (RP) and a barrel-shaped 20S core particle (CP), which together form the 26S proteasome (**Figure 3.5.1.1**). The 20S proteasome alone is capable of degrading oxidized and otherwise structural disordered proteins (Ben-Nissan and Sharon, 2014; Davies, 2001). The core particle is composed of four axial heteroheptameric rings, two outer α- and two inner β-rings. These rings consist of seven subunits each (Dong et al., 2019; Tomko and Hochstrasser, 2013).

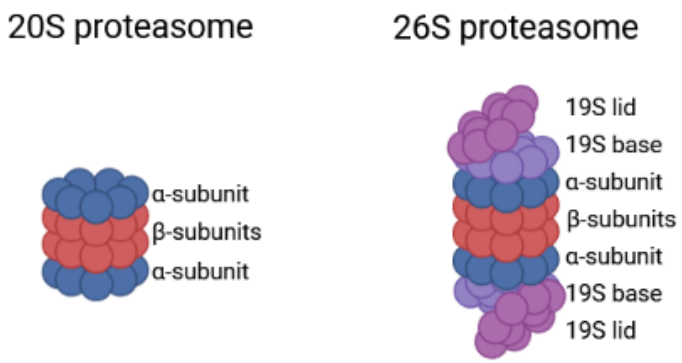

Figure 3.5.1.1: The difference between the 20S and 26S proteasome. The 20S proteasome consists of two inner β-subunits with the catalytical units, while the α-subunits form the entrance ring. The 26S proteasome consists additionally of the 19S regulatory particle, which in turn consists of the base and lid. Graph was designed with BioRender.com.

The α-subunits form a ring (or gate), which allows tight regulation of entrance of the substrates. The mechanism of opening the "gate" and proteasome activity are regulated by certain proteins, such as 19S RP, PA28, PA200 and ECM29. These proteins have a HbYX motif in common (where Hb stands for hydrophobic residue, Y for tyrosine and X for any amino acid). These proteins bind onto seven binding pockets formed by α-α interfaces on the 19S RP facing

the surface of the outer α-rings. The inner β-rings also have seven distinct subunits (β1-7), which are flanked by the two outer α-rings. Three of these subunits contain one active site with a different proteolytic specificity. These proteolytic sites are caspase-like, trypsin-like and chymotrypsin-like (Bochtler et al., 1999; Livneh et al., 2016; Sauer and Baker, 2011; Yedidi et al., 2017). The different proteolytic sites prefer distinct amino acids. The caspase-like site prefers acidic amino acids, while the trypsin-like site prefers basic amino acids and the chymotrypsin-like site prefers hydrophobic amino acids. Since there are two β-subunits, each 20S proteasome has six catalytically active sites.

The 19S RP is a multifunctional complex, which regulates the activity of the proteasome. Its functions are identification of substrates to be degraded as well as binding, deubiquitylation, unfolding and translocation of substrates into the proteolytic chamber of the CP. The 19S RP is further divided into the “base” and the “lid”. The base consists of six regulatory ATPase subunits (Rpt1-6), which are organized into a ring, and four regulatory non-ATPase subunits (Rpn1, Rpn2, Rpn10 and Rpn13). These non-ATPase subunits serve as ubiquitin receptors, which recognize ubiquitinated proteins marked for degradation (Livneh et al., 2016; Sauer and Baker, 2011; Yedidi et al., 2017). The lid consists of nine different regulatory particle non-ATPases (Rpn) subunits (Rpn3, Rpn5-9, Rpn11, Rpn12 and Rpn15), which form a horseshoe shaped structure. The main function of the lid is the deubiquitylation of incoming substrates, which is carried out by deubiquitylating enzymes (DUBs), such as Rpn11, Uch37 and Ubp6/Usp14 (Livneh et al., 2016; Yedidi et al., 2017).

4.5.2. Ubiquitin degradation pathway

The best studied degradation pathway is the ubiquitin degradation pathway. It basically consists of two parts: the covalent binding of ubiquitin to proteins, which are to be degraded, and the degradation by the 26S proteasome. The process of adding ubiquitin to a protein is termed ubiquitylation and is catalyzed by the ubiquitin-activating enzyme E1. The reaction is ATP-dependent and links the ubiquitin C-terminus (Gly76) to the active site cysteine residue of the E1 in a high-energy thioester linkage reaction. Ubiquitin is then transferred from the E1 to an active site cysteine residue of the ubiquitin-conjugating enzyme E2. Finally, the ubiquitin ligase E3 mediates the interaction between the E2-ubiquitin and the target protein, stimulating the transfer of the ubiquitin chain(s) to the target protein. The chains are usually transferred to lysine sidechains of the target protein (**Figure 3.5.2.1**) (Deshaies and Joazeiro, 2009; Hochstrasser, 1995; Mehrtash and Hochstrasser, 2019). The proteins marked for proteasomal degradation typically contain at least one poly-ubiquitin chain (of at least four ubiquitin molecules) or multiple mono-ubiquitin additions.

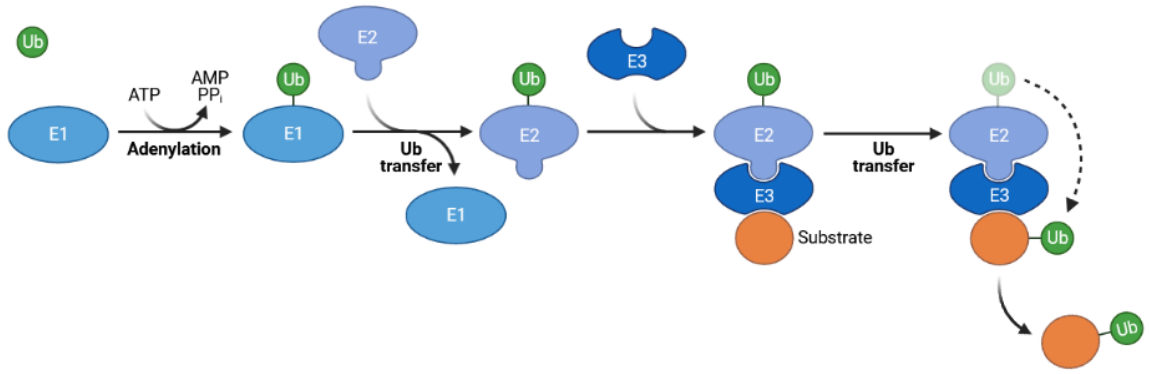

Figure 3.5.2.1: The ubiquitin transfer machinery. The ubiquitin-activating enzyme E1 hydrolyses ATP to activate ubiquitin and transfers it to the ubiquitin-conjugating enzyme E2. The ubiquitin-ligase E3 is transferring the ubiquitin to the target substrate. The figure was created with BioRender.com.

There are three proteasomal subunits, which have been shown to bind ubiquitinated proteins: Rpn1, Rpn10 and Rpn13 (Hochstrasser, 1995; Livneh et al., 2016; Mehrtash and Hochstrasser, 2019). Rpn13 binds ubiquitinated substrates via its N-terminal pleckstrin-like receptor of ubiquitin domain, while its C-terminal domain is known to bind and activate the DUB Uch37. Together they function as proof-reading or editing machinery that enables the escape of poorly or inadvertently ubiquitinated substrates by removing their ubiquitin moieties. In other cases, the ubiquitin chain might be trimmed to a length that fits the proteasome better, directing the substrate for efficient degradation (Livneh et al., 2016; Mehrtash and Hochstrasser, 2019; Yedidi et al., 2017). The poly-ubiquitin chain is then hydrolyzed by Rpn11 and then stripped of the protein. ATP hydrolysis triggers conformational changes of individual ATPase subunits that cause a pulling force and start the unfolding and translocation of the target protein through the narrow gate of the proteasome. The α-rings are consecutively widened to adopt to the unfolding polypeptide chain. The unfolded polypeptide chain is then degraded into ~10 amino acid long residues by the catalytically active pockets (Bard et al., 2018; Inobe et al., 2011). The hydrolysis rate of the proteasome during this process is ~30-50 molecules of ATP per minute (Kim et al., 2015).

4.6. Degrons

Degradation signals or degrons are features of short-lived proteins. The first identified degradation signals were termed degrons and found at the N-terminus of short-lived proteins. Analysis of these degrons, and their motifs, was later termed the “N-end rule” (Varshavsky, 2011). Degrons can also occur at the C-terminus. While these degrons differ from the N-

terminal ones mechanistically and location-wise, they are analogous to N-degrons in the degradation pathway. In the following paragraph, I will give a short overview about N-terminal and C-terminal degrons.

4.6.1. N-terminal and C-terminal degrons

The N-degron pathway combines a set of proteolytic systems, that is characterized by a destabilizing residue at the N-terminus of a protein. These proteins are either degraded by the proteasome in human cells or the ClpAP protease in bacteria (Dougan et al., 2012; Varshavsky, 2019). Some N-degrons are first masked by different residues and need processing before they are recognized. Exopeptidases, such as the mammalian DPP9, can convert pre-N-degrons to N-degrons by cleavage of specific amino acids at the N-terminus (Justa-Schuch et al., 2016). Consequently, many amino acid combinations can have a destabilizing effect on a protein in the right context. These degrons limit the half-life of many proteins in the cell by targeting them for degradation via N- or C-terminal degrons. The N-degron pathway shows a certain variety. There are the Arg/N-, the Ac/N-, the Pro/N- and the Gly/N-degrons (Timms and Koren, 2020; Varshavsky, 2019, 2011). The different variants of these pathway have in common, that the N-terminal residue is recognized by proteins called N-recognins. The same is true for C-terminal residues and C-recognins. In mammalian cells these recognins often belong to the family of ubiquitin protein ligase E3 component N-recognin 1 (Ubr) proteins (Tasaki et al., 2005; Tasaki and Kwon, 2007; Timms and Koren, 2020; Varshavsky, 2019). Once a specific N-terminus is presented, e.g. ArgCysGln, a recognin binds the sequence and initiates its ubiquitylation. Once ubiquitylated, the protein is marked for degradation by the proteasome. These N-degrons can also be part of a quality control, since not correctly folded or otherwise aberrant amino acids can induce degradation (Timms and Koren, 2020). In some cases, a cleavage of the initial methionine can reveal such a degron. An example for this case is the Pro/N-degron pathway. The initial sequence of a protein might consist of methionine at the first and proline at the second position. After cleavage with METAP1/2 the proline is recognizable for the glucose-induced degradation E3 ubiquitin ligase complex. The ubiquitin ligase then adds ubiquitin to the protein and marks it for degradation (Dougan et al., 2012; Timms and Koren, 2020; Varshavsky, 2019).

Other examples of N-terminal sequences, which mark a protein for degradation, are the β-galactosidase degron WRFAAWFP or the UmuD degron consisting of an FPLF degron in the first 15 amino acids. These two degrons are recognised by the Lon protease in prokaryotes (Gonzales et al., 1998; Gur and Sauer, 2009, 2008). They are probably recognized by their

hydrophobic amino acids, which usually occur in the protein core and are masked by their structure. The occurrence of hydrophobic amino acids in unstructured regions might be interpreted by the cell as an insufficiently folded protein. These unfolded proteins then activate the unfolded protein response and mark a protein for rapid degradation (Braunstein et al., 2015; Strub et al., 2004; Wetzel, 1994). A similar degron containing hydrophobic amino acids was discovered by me in the MAX isoform E protein, although these amino acids reside at the C-terminus (Peter et al., 2021).

Known C-terminal degrons contain a PxxP, RG or RxxG motif in eukaryotes. Most C-terminal degrons in eukaryotic cells are recognized by the E3 ubiquitin ligase cullin-RING (CRL) family (Koren et al., 2018; Lin et al., 2018; Varshavsky, 2019). This family recognizes short (six to ten) amino acids long residues at the C-terminus, which indicate a truncated protein. Indeed most found proteins in the study were truncated due to cloning errors of the used library (Lin et al., 2018). Nonetheless it was found, that essentially degrons containing an RxxG, RG or GG motif are recognized by CRL2. As indicated by the sequence, a C-terminal glycine plays a critical role in this recognition process. This E3 ligase is marking the recognized protein with ubiquitin, which then is degraded by the 26S proteasome (Koren et al., 2018; Lin et al., 2018). The PxxP motif was found in the context of AS within the 3'-UTR or frameshifting-induced skipping of internal exons. This process can generate a stop codon in the following exon (Preussner et al., 2020). The frameshift or AS event also causes an enrichment of proline, cysteine, serine and leucin. While cysteine is a known target for oxidation (Davies, 2001; Dissmeyer et al., 2018), the enrichment of proline at the C-terminus correlates with intrinsic protein disorder (Preussner et al., 2020). The occurrence of hydrophobic amino acids, such as leucine, phenylalanine or tryptophan at the C-terminus might indicate an unproperly folded protein and is thus a degradation signal (Braunstein et al., 2015; Peter et al., 2021; Preussner et al., 2020).

In prokaryotic cells the membrane-anchored protease FtsH is the only essential protease in *E. coli* (Langklotz et al., 2012). Prokayrotic C-terminal degrons include the AVLA motif of LpxC protein or the LSGL motif of the model substrate titin^{I27}(Führer et al., 2007; Gur and Sauer, 2009; Koren et al., 2018; Preussner et al., 2020). The FtsH protease recognizes amongst other things proteins with a C-terminal degradation signal AAXXXXXALAA-tag (SsrA-tag). The adjustsment of the cellular amount of UDP-3-O-(R-3-hydroxymyristoyl)-N-acetylglucosamine deacetylase (LpxC) is important for lipopolysaccharide biosynthesis. Its accumulation or depletion is toxic for *E. coli* and thus, LpxC needs to be tightly regulated.

4.7. Impact of mRNA structures on gene expression

In recent research the mRNA structure is more and more considered to have an impact in posttranscriptional gene regulation (Lewis et al., 2003). Structures can block accessibility of *cis*-regulatory elements by masking them for *trans*-acting factors. This indicates, that RNA structure can influence the strength of regulation by modulating the affinity of *trans*-acting factors to the required binding site. In addition, some RBPs are able to identify and bind directly to certain RNA structures, either via dedicated domains, like double stranded RNA binding domains, or via classical single stranded RNA binding domains, which may have a preference for the presentation of their binding sequence within a stem-loop (SL) structure (Dominguez et al., 2018; Lewis et al., 2003). One example of an RBP binding specifically to the shape of an RNA is the protein Roquin with its ROQ-domain. Structures are also prevalent in viral RNAs and are essential for viral replication (Madhugiri et al., 2018; Manfredonia and Incarnato, 2021).

4.7.1. Roquin

The Roquin protein family consists of two paralogs, Roquin-1 and Roquin-2, which are two RBPs regulating immune homeostasis. Roquin-1 was initially found by mouse mutagenesis screens for regulators of autoimmunity. Mutation of the *RC3H1* gene, which encodes the Roquin-1 protein, caused the development of a T follicular helper cell-driven lupus-like autoimmune disease. The disease is induced by the activation of T cells and the resulting and accumulation of T follicular helper cells and their production of antibodies (Vinuesa et al., 2005; Yu et al., 2007). The effect was due to the missing regulation of certain Roquin targets. These Roquin targets are inducible T-cell costimulatory (*ICOS*), *CTLA4*, *OX40*, the cytokines *TNF* and *IL6*, the transcription factors *IRF4* and *c-Rel*, and modulators of transcription *NFKBID* and *NFKBIZ* (Essig et al., 2018; Murakawa et al., 2015; Vogel et al., 2013).

Roquin-1 and Roquin-2 seem to have redundant functions in regulation gene expression. They share around 80% sequence identity in their N-terminal region, which contains the unique ROQ-domain, with which Roquin proteins recognize RNA structures. Further, Roquin proteins posses a CCCH-zinc finger domain, which might contribute to RNA binding. The C-terminus is predicted to be intrinsically disordered and contains a proline-rich stretch for protein-protein interactions (Figure 3.7.1.1) (Schaefer and Klein, 2016; Schlundt et al., 2016). The function of the C-terminus consists of the recruitment of the CCR4-CAF1-NOT deadenylation machinery and the subsequent degradation of target mRNAs (Leppek et al., 2013). Binding of Roquin to target mRNA usually results in posttranscriptional repression through mRNA decay (Sgromo et al., 2017).

It was shown, that Roquin recognizes and binds 3'-UTR structures such as SLs with a tri-nucleotide loop (Braun et al., 2018; Janowski et al., 2016; Tan et al., 2014). These SL structures are called constitutive decay elements (CDEs). The most studied CDE is the initially discovered *TNF* CDE. Mutational analysis of the *TNF* CDE showed a strong preference of Roquin to bind pyrimidine-purine-pyrimidine (Y-P-Y) tri-nucleotide loops, whereby the stem has two pyrimidine-purine (Y-P) closing base pairs (Leppek et al., 2013). This binding motif however hadto be revised, as more and more Roquin binding sites were identified (Binas et al., 2020; Braun et al., 2018; Rehage et al., 2018; Schlundt et al., 2016). Braun et al. identified a preference for Roquin to bind Y-P-N triloop SLs, while there is a preference for uridine at the third position in mammalian cells (Figure 3.7.1.1). Further, there are no preferences for specific base pairs in the stem region(Braun et al., 2018). By structure prediction a plethora of new Roquin binding targets could be identified, twelve of them were verified by Roquin knockdown in HEK293 and HUVEC cells. Interestingly, several of the newly identified CDEs were AU-rich or even completely composed of A und U residues. As, AU-rich elements (AREs) are well-known mRNA decay elements, we hypothesized that AU-rich CDEs could have a dual function in mRNA decay. Dependent on their folding status, they might either be recognized by Roquin proteins or by proteins binding to single stranded AU-rich sequences (Binas et al., 2020).

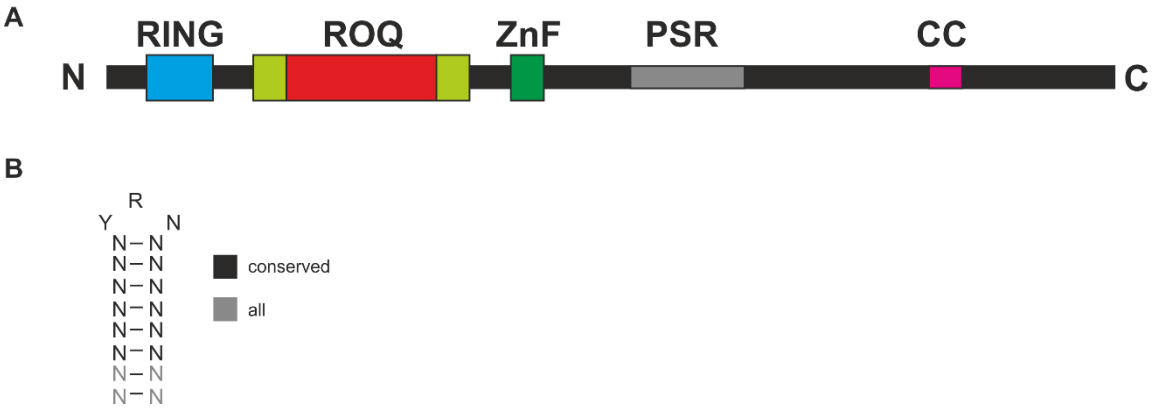

Figure 3.7.1.1: Roquin domain scheme and preferred binding pattern. (A) Roquin-1 consists of a N-terminal RING (really interesting new gene) domain, followed by a ROQ and zinc finger (ZnF) domain. The Proline-Serine-Rich domain (PSR) and the coiled coil (CC) domain are close to the C-terminus. **(B)** Roquin-1's preferred CDE binding structure. The letters marked black are conserved between mammals, while the grey ones are non-conserved CDEs.

4.8. SARS-CoV-2

SARS-CoV-2 (severe acute respiratory syndrome coronavirus 2, SCoV2) belongs to the β-coronaviruses and is the causative agent of COVID-19 (coronavirus disease 2019). It is the third highly pathogenetic, zoonotic virus from this genus. SCoV2 belongs to the

Orthocoronavirinae subfamily, which has four genera, namely α-, β-, γ- and δ-coronaviruses. α- and β-coronaviruses (CoVs) are able to infect humans, which usually results in respiratory illnesses, while the β-CoVs comprise three of the most pathogenic CoVs (Cui et al., 2019) The first was SARS-CoV (SCoV1), which originated from bat and civet cat back in 2002/3. The second was MERS (middle east respiratory syndrome)-CoV, which originated from camels (Čivljak et al., 2020; Wang et al., 2020). The third now SCoV-2. The genome sequence homology between SCoV2 and SCoV1 is estimated to be ~79% (Romano et al., 2020; Wang et al., 2020).

SCoV2 viruses are enveloped, positive sense, single stranded RNA viruses. The exceptionally large viral genome is ~30 kb in length (Kumar et al., 2020). The large genome directly acts as mRNA in the cytoplasm and encodes ~28 viral proteins. The virus contains 14 ORFs, while the two main transcriptional units, ORF1a and 1b, encode the polyprotein 1a (PP1a) and polyprotein 1b (PP1b). These polyproteins embed non-structural proteins (Nsp1-16), which form the complex replicase machinery (Romano et al., 2020; Wang et al., 2020). The complete structure of the virion consists of mainly four components: spike (S), nucleocapsid (N), membrane (M) and envelope (E) (**see Figure 3.7.1.1**). The

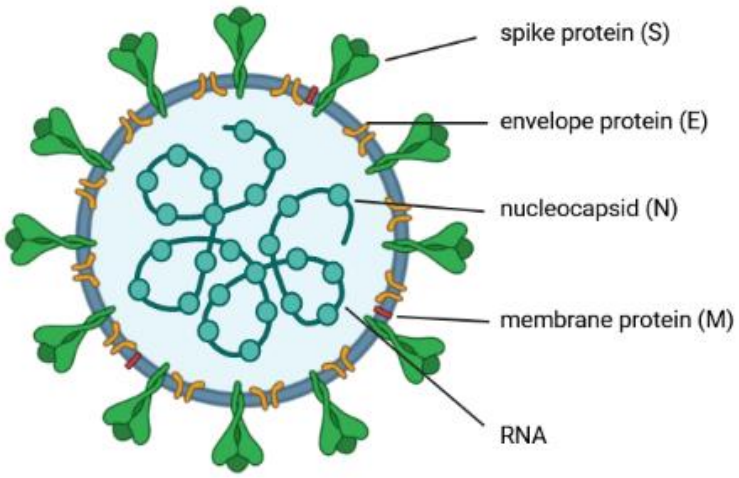

Figure 3.7.1.1: Schematic structure of SCoV2. Green structures indicate the spike protein (S), yellow the envelope protein (E), red the membrane protein (M), light blue circles the nucleocapsid (N) and the dark blue line indicates the genomic RNA. Figure was designed by BioRender.com

4.8.1. Structure of the RNA genome of SCoV2

The RNA genome of the virus contains not only the coding regions for viral proteins, but also highly structured 5'- and 3'-UTRs, as well as internal structured RNA elements with essential functions in genome replication, transcription of subgenomic (sg) mRNAs and the balance translation synthesis of viral proteins (Das et al., 2021; Kumar et al., 2020; Rangan et al., 2021).(Kelly et al., 2020; Madhugiri et al., 2016; Tidu et al., 2021). The structures of the 5'-UTR extend into the first open reading frame (ORF) and contain eight stem-loops (SLs), while the 3'-UTR contains three, a stem-loop II-like motif (s2m) and a hypervariable region (HVR). In between two reading-frames, ORF1a and 1b, is an attenuator hairpin followed by a pseudoknot (PK) (see **Figure 3.7.1.1**).

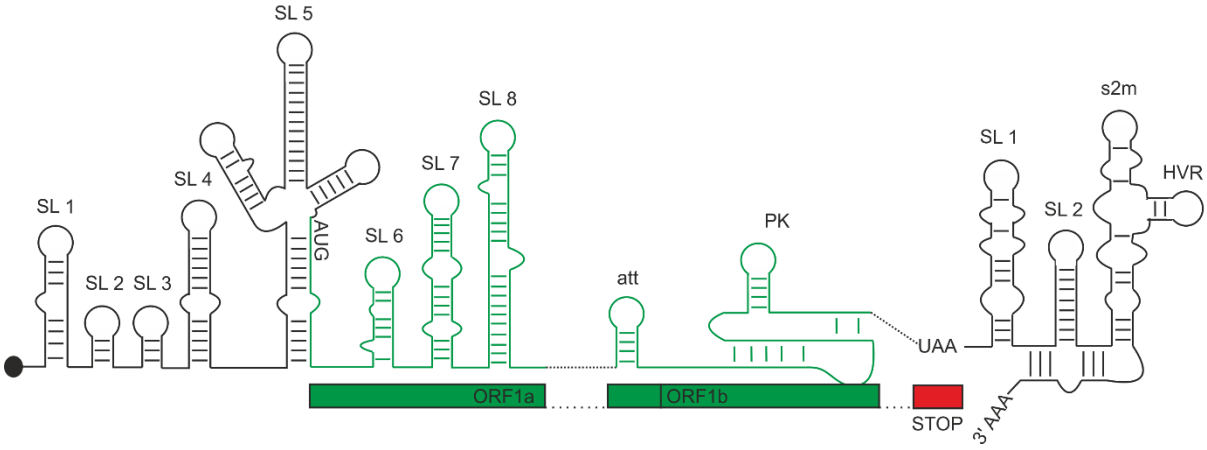

Figure 3.7.1.1: Scheme of the structured RNA elements in SCoV2. Green lines indicate RNA structures in ORFs. The green boxes and lines indicate the ORF1a or 1b respectively. Red box indicates the stop codon. SL indicates stem-loop, att indicates the attenuator hairpin, PK indicates pseudoknot. HVR indicates hyper-variable region, s2m indicates stem-loop II-like motif.

Phylogenetic comparison of the RNA structures of different coronaviruses (CoVs) revealed an importance in the RNA elements shown in Figure 3.7.1.1. The SLs are conserved between different β-coronaviruses, which highlights their importance in the viral life cycle(Chen et al., 2021; Chen and Olsthoorn, 2010).

SLs in the 5'-UTR: SL1 from the 5'-UTR has a functionally bipartite structure, where the upper part must be folded. Destabilization experiments introduced into SL1 of mouse hepatitis virus (MHV), a well-studied model for betacoronaviruses, leads to defects in viral replication. Replication could be rescued by compensatory mutations, which restore the base-pairing (Li et al., 2008). In contrast, the lower part of SL1 needs to be structurally dynamic for long-range interactions with the 3'-UTR to enable the synthesis of subgenomic mRNA (sgmRNA). Studies conducted in MHV and the human-transmissible α-coronaviruses 229E and NL63 (HCoV229E

and HCoVNL63) showed, that mutations in the lower part of SL1 cause defective sgRNA synthesis (Madhugiri et al., 2018). The SL1 appears to be structurally conserved, since replacement of MHV SL1 with SARS-CoV1 SL1 yields viable chimeric viruses (Kang et al., 2006). SL2 is a highly conserved *cis*-acting structure with functional relevance (Chen et al., 2021; Kang et al., 2006). Mutations disrupting SL2 lead to impaired sgRNA synthesis in MHV (Liu et al., 2007). Similarly, replacement of SL2 of HCoV229E with bovine CoV or SCoV1 yielded vital and functional virus chimeras. These chimeras were comparable in infectivity to the wild-type HCoV229E and therefore indicate a structural and functional conservation of SL2 (Madhugiri et al., 2018; Manfredonia and Incarnato, 2021). SL3 is conserved in only a small subset of β- and γ-CoVs. When the structure is present, as shown for SCoV1 and SCoV2, it encompasses the transcription regulatory sequence, which is essential for the synthesis of the sgmRNAs. In most other CoV the transcription regulatory sequence is predicted to be single stranded, such as in MHV. Recent results indicate, that the SL3 in SCoV2 might undergo dynamic unfolding in order to mediate genome cyclization. Direct capture of *in-vivo* RNA-RNA interactions further support this model (Manfredonia and Incarnato, 2021). SL4 consists of a bipartite hairpin separated by an internal loop and is conserved in all CoV genera. SL4 contains an upstream ORF (uORF), which is conserved in 75% of β-CoVs. This uORF encodes for a polypeptide of 3 to 13 amino acids. Mutations disrupting the coding potential of the uORF in MHV, while maintaining the RNA structure, resulted in increased translation of ORF1ab. These mutations were rapidly reverted. Complete deletion of the uORF start codon resulted in defective viruses and was spontaneously rescued by the appearance of a new uORF (Yang et al., 2011). This finding suggests a role in the regulation of the translation of ORF1ab. A complete deletion of SL4 was lethal for the virus. SL5 contains the start codon of the ORF1ab and is conserved in both α- and β-CoVs (Chen et al., 2021; Manfredonia and Incarnato, 2021). It consists of a four-way junction with three substructural SLs, SL5A, SL5B and SL5C (Chen et al., 2021; Manfredonia and Incarnato, 2021; Wacker et al., 2020). The loops of SL5A and SL5B are identical and conserved across nearly all α- and β-CoVs, which highlights their importance in viral replication. The loop consists of a 5'-UUYCGU-3'-motif (Chen et al., 2021; Schnieders et al., 2021). The structure of SL5 has been experimentally confirmed *in vivo* and *in vitro* (Huston et al., 2020; Manfredonia and Incarnato, 2021; Wacker et al., 2020). The importance of SL5A is highlighted by disruption experiments. Disrupting of SL5A causes impairment of viral replication in MHV (Manfredonia and Incarnato, 2021). It is therefore thought, that SL5 might be involved as a signal for genome packaging in CoVs, but the exact mechanism is not yet understood (Chen et al., 2021; Masters, 2019). A number of additional of SLs, SL6-8, have been found in the ORF1a, which might also function in viral replication. SL6 and SL7 has been proven to exist in MHV by *in vitro* and *in vivo* probing and SL6- 8 have been shown to be structured in SCoV2 (Manfredonia and Incarnato, 2021; Wacker et al.,

2020). However, they seem to be less conserved and their function could not yet be determined (Madhugiri et al., 2018; Manfredonia and Incarnato, 2021).

Most knowledge on the 3'-UTR of coronaviruses comes from studies conducted on β-CoVs. The region is indicated to be structurally and functionally conserved within the same genus, e.g. demonstrated in that the complete 3'-UTR of SCoV1 can be functionally replaced with that of MHV (Chen et al., 2021; Manfredonia and Incarnato, 2021). The most proximal structure after the ORF is SL1, which has a high structural, but low sequence conservation across β-CoVs (Chen et al., 2021; Manfredonia and Incarnato, 2021; Wacker et al., 2020). This structure seems to be involved in the regulation of replication and it has been proposed, that it might act as an molecular switch in combination with a pseudoknot structure formed with SL2 of the 3'-UTR (Chen et al., 2021; Goebel et al., 2004; Wacker et al., 2020). In α-CoVs, the structure of SL1 of the 3'-UTR seems not to be present, although the pseudoknot is predicted to exist. Its formation appears to be mutually exclusive with the presence of a small upstream SL, which indicates the existence of the same switch in α-CoVs (Madhugiri et al., 2016). The downstream structure of the 3'-UTR is known as the hypervariable region (HVR). The HVR sequence is poorly conserved, albeit an octanucleotide 5'-GGAAGAGC-3', while the structure is highly conserved across all CoV genera (Madhugiri et al., 2018; Manfredonia and Incarnato, 2021). The exact function still needs to be assessed. Although deletion of the whole structure causes a loss of pathogenicity in MHV, extensive mutation seems to be widely tolerated (Manfredonia et al., 2020; Ziv et al., 2020). The HVR contains the structured s2m motif, which is highly conserved across all β-CoVs. The s2m sequence and structure are highly important for virus replication, since mutations can be lethal or lead to short-lived viruses (Chen et al., 2021; Gilbert and Tengs, 2021; Manfredonia et al., 2020; Wacker et al., 2020). The loop consists of a GAGUA motif and has been proven under several conditions *in vitro* and *in vivo* (Chen et al., 2021; Kumar et al., 2020; Manfredonia and Incarnato, 2021; Wacker et al., 2020).

4.8.2. Frameshifting element

Located in between ORF1a and ORF1b is the well conserved ribosomal frameshifting element (FSE), which regulates a programmed -1 ribosomal frameshift. The frameshift is enabling the translation of ORF1b, which partially overlaps with ORF1a. In CoVs, it generally consists of a slippery sequence 5'-UUUAAAC-3' followed by a single stranded spacer and a pseudoknot structure (PK) (Bhatt et al., 2021; Kelly et al., 2020; Manfredonia and Incarnato, 2021; Rangan et al., 2021). The pseudoknot consists of two stacked stems, connected with two large loops. SCoV1 and SCoV2 have an additional structure, which is located directly upstream of the slippery sequence. The structure is an attenuator hairpin (att HP) and has been reported to

regulate the programmed ribosomal frameshift (Kelly et al., 2020; Manfredonia and Incarnato, 2021; Rangan et al., 2021; Wacker et al., 2020). Maintaining the precise level of CoV frameshifting efficiency is crucial for viral infectivity. Indeed, mutations of a single nucleotide in the frameshifting region of SCoV1 RNA almost completely ablates viral propagation and reduced viral infectivity by > 3.5 orders of magnitude (Plant et al., 2010).

5. Aim of this work

Overall, in this thesis novel post-transcriptional gene regulation mechanisms were characterized: Aim 1 was to unravel by which mechanism a previously described alternative splicing event elicits protein degradation. Aim 2 was to investigate if AU-rich RNA structures might serve a dual function in gene repression and Aim 3 was to characterize RNA structures in the genome of SCoV2 and thus lay the basis for structure-based drug discovery.

Aim 1 was the characterization of the mechanism underlying the rapid degradation of *MAX* isoform E. *MAX* isoform E harbors 36 alternative amino acids at its C-terminus, which cause rapid degradation of the protein. I wanted to pinpoint the amino acids responsible for the degradation mechanism and if this mechanism is conserved between different species. To achieve this aim, I successfully tested the efficiency of different mutations in different organisms and identified the involved proteases. The data are published (Peter et al., 2021).

Aim 2 was the analysis of AU-rich CDEs in the 3'-UTR of *UCP3*. Structured *cis*-regulatory elements in the 3'-UTR of RNA are used to build up complex genetic circuits. AREs are short linear motifs with a high content of complementary A and U nucleotides and often occur in multiple copies. This project consisted of two parts: First, we wanted to confirm the recognition of the AU-rich RNA element by Roquin as SL. Second, we wanted to test the competition of Roquin with AUF1 as a representative for an RBP, which recognizes AU-rich ssRNA elements. The data are published (Binas et al., 2020).

Aim 3 of this study is the folding of the 5'- and 3'-UTR structures of SCoV2. SCoV2 belongs to the class of β-*coronaviridae* and causes a worldwide pandemic. α- and β-*coronaviridae* have extensively structured 5'- and 3'-UTRs, which are linked to viral replication and pathogenicity. The third project involves two parts: First, we wanted to determine the fold of the functional *cis*-elements in the genome of SCoV2. Second, we wanted to use this information for the development of small molecules for inhibition against specific RNA structures. The data are published (Schnieders et al., 2021; Sreeramulu et al., 2021; Vögele et al., 2021; Wacker et al., 2020).

6. Discussion

In this thesis, I was able to characterize novel post-transcriptional regulation mechanisms in three interrelated projects:

1) I was able to identify a protein degradation mechanism coupled to alternative splicing, which is termed AS-CPD. This mechanism was discovered by an alternative splicing event, where the last intron is retained. The alternatively added amino acids contained a powerful degradation tag, called isoE C-degron. The degron dramatically reduced the half-life of fusion proteins and showed full activity in *E. coli*, *S. cerevisiae* and mammalian cells. The important amino acids for the function of the degradation tag are phenylalanine and tryptophan. In the discussion, I will compare the degradation signal to previously known degradation pathways and speculate on a possible universal mechanism involving the degradation signal. Then I will discuss possible functions of the discovered regulation mechanism.

2) We were also able to identify an ARE-like function of AU-rich CDEs. The first CDE in the 3'-UTR of *UCP3* consists of an AU-rich element, which is recognized as a SL by of Roquin, but can also be bound in its linear form by AUF1. This mechanism adds an additional layer to the regulation of mRNA half-life mediated by its 3'-UTR. I will discuss how the competition of RBPs for binding sites affect regulation. Furthermore, I will discuss the potential of transient structure formation in AU-rich elements for gene regulation.

The last aim of the work was the characterization of structured elements in SCoV2 RNAs. The SCoV2 genome has extensively structured 5'- and 3'-UTRs as well as a frameshifting element. We were able to provide detailed structure information for 15 RNA elements and found that most of them were addressable by small chemical components. The inhibition of RNA structural elements via small molecules can provide a novel, alternative approach for medical treatments of patient suffering from COVID-19. In the discussion, I will provide a rough overview of currently used therapeutics against Covid-19 in the light of possible RNA drugs, such as antisense oligonucleotides or small molecules. The latter will be discussed with the example of screenings against the pseudoknot structure of SCoV2.

6.1. Aim 1: Characterization of the coupling between pre-mRNA splicing and protein degradation

6.1.1. Alternative splicing coupled to protein decay (AS-CPD)

We recently discovered a new mechanism involving alternative splicing. During this process, the last intron is retained, which creates a truncated protein with a different C-terminus. The alternate C-terminus contains a strong degradation signal, which caused rapid degradation in

mammalian cells, *S. cerevisiae* and *E. coli*. This indicates a universally conserved mechanism. The amino acids, which are responsible for the recognition and fast degradation, are hydrophobic amino acids such as phenylalanine and tryptophan. A mutation replacing those two with alanine resulted in higher protein levels, resulting in a prolonged protein half-life. In contrast, mutation to leucine and isoleucine did not change the degradation efficiency compared to alanine. Leucine and isoleucine are equally hydrophobic compared to phenylalanine and tryptophan. Hydrophobic amino acids are generally in the interior of a properly folded protein and the occurrence on the outside indicates a misfolded protein for the cell (Strub et al., 2004). To prevent the accumulation of misfolded and therefore dysfunctional proteins, the misfolded proteins have to be degraded (Balchin et al., 2016; Wetzel, 1994). The accumulation of misfolded proteins is toxic for the cell, reduces the concentration of active proteins and promotes inclusion bodies (Balchin et al., 2016), which in turn has a strong impact on the human body causing for example neurodegenerative diseases, such as Alzheimer's or Parkinson's (Schmidt and Finley, 2014; Zheng et al., 2016). Hence, the cell needs to get rid of unfolded proteins as fast as possible. A possible way to degrade unfolded proteins is the unfolded protein stress response (UPR) by the endoplasmic reticulum (ER). The UPR can increase the turnover rate and therefore increase degradation detecting unfolded proteins via three different pathways involving the following proteins: inositol-requiring enzyme 1 (IRE1), protein kinase RNA-like ER kinase (PERK) and activating transcription factor 6 (ATF6). In mammalian cells, IRE1 is a transmembrane protein, where its N-terminus reaches inside the lumen. The N-terminus can interact with unfolded proteins, while the C-terminus lies in the cytosol and contains a serine-threonine kinase and an endoribonuclease domain (Hernández-Elvira et al., 2018; Karagöz et al., 2019; Vembar and Brodsky, 2008). If an unfolded protein is bound by IRE1, it undergoes a conformational change, which recruits chaperones. If these chaperones are unable to properly fold the protein, E3 ubiquitin ligases are recruited, which mark the potentially unfolded protein with ubiquitin. These marked proteins are then relocated by the Cdc48 complex and then transported to the 26S proteasome for degradation (Karagöz et al., 2019; Vembar and Brodsky, 2008). The same degradation pathway might apply to the mechanism I found in human cells.

The UPR pathway also exists in yeast cells, although the only sensor for unfolded proteins is the IRE1 protein. IRE1 is also membrane bound in yeast cells and undergoes a conformational change after unfolded proteins are bound. This conformational change releases the chaperone BiP and the transcription factor Hac1. Hac1 upregulates a variety of genes, which involve chaperones, post-transcriptional modification enzymes and proteasomes, such as the Hsp70 protein family (Hernández-Elvira et al., 2018). The isoE degron is likely to be degraded via by the proteasome in a stress mediated pathway to counteract the accumulation of misfolded proteins (Geiler-Samerotte et al., 2011; Hiller et al., 1996).

Although *E. coli* does not have a proteasome such as eukaryotic cells, it has a similar mechanism coping with UPR. In *E. coli* unfolded proteins are sensed by outer membrane porins (OMPs). These OMPs undergo a conformational change and bind to the inner membrane bound protease DegS. DegS is then activated and cleaves a complex consisting of RseA, RseB and the transcription factor SigmaE. RseA is then cleaved off and a complex of RseA and SigmaE is released into the cell lumen. The complex is then recognized by the protease ClpXP and RseA is degraded (Tomoyasu et al., 2001). SigmaE can now bind the RNA polymerase core enzyme and redirect it to transcribe more RNA of chaperones or proteases to cope with unfolded protein stress (Truscott et al., 2011). However, I could not detect any difference in the degradation with the ClpXP knock-out strain, which indicates no function of ClpXP in the mechanism I found. In some cases it is reported, that other proteases, such as the Lon-protease can be upregulated in its activity to cope with unfolded protein stress (Tomoyasu et al., 2001; Truscott et al., 2011). The degradation motif of the isoE C-degron consists of FxxW, which we could show to be a target for Lon-mediated decay, as it preferably degrades proteins carrying hydrophobic amino acids (Gur et al., 2012; Gur and Sauer, 2008). In contrast to that, the ClpXP protease recognizes proteins containing two C-terminal alanine and the negatively charged α-carboxylgroup (Baker and Sauer, 2012). Taken together, there are dedicated mechanisms to recognize unfolded proteins in all three organisms, which could explain the universal degradation activity of the isoE-degron.

6.1.2. Evolution of the proteasome

Nonetheless, the question remains, if the proteases, which are responsible for the degradation of the isoE C-degron have any evolutionary link. While the 20S proteasome is ubiquitously expressed in eukaryotes and a more primitive form in archaea, only a small range of bacteria have evolved a multifaceted protein degradation machinery (De Mot, 2007; Jastrab and Darwin, 2015). Bacteria have generally evolved unrelated proteases, such as the ClpP, Lon or FtsH protease, but also proteasome homologs. One homolog for example is the HslV protease, which consists of a dodecamer of two hexameric rings and in combination with the AAA unfoldase HslU forms the HslUV protease complex (Sauer and Baker, 2011). The HslV protease relies in its recognized motif on N-terminal serine or threonine residues as the catalytic nucleophile. There are two more proteases identified with a similar structure and degradation mechanism, which recognizes N-terminal nucleophiles (NTNs). These 2 proteases are the ancestral β-subunit (Anbu) and the β-proteobacterial proteasome homolog (BPH) (Fuchs et al., 2017; Piasecka et al., 2018; Vielberg et al., 2018). A defining feature of the proteasome family across the different species, is the double-ring architecture of their catalytic subunit. Recent bioinformatic analyses suggest that Anbu and the proteasomal

β-subunit have a shared ancestry in the last universal common ancestor, while the Anbu architecture resembles the common precursor (Fuchs and Hartmann, 2019). These precursors exist in different conformations via lateral or helical association and the Anbu is found in different states in different organisms. So far, both dodecameric assemblies consisting of six and tetradecameric assemblies consisting of seven dimers have been found (Fuchs et al., 2017; Piasecka et al., 2018; Vielberg et al., 2018). One key element in the formation of protomers to a helical coiled coil formation is the C-terminal helix. If the C-terminal helix is too short or truncated, the coiled coil formation is not possible to form (Fuchs and Hartmann, 2019). In consequence, the α-subunits are necessary for higher stable ring formations, such as the proteasome possesses. The shortening of the C-terminal helix probably lead to the diversification of the proteo β subunit into differentiated α- and β-subunits and the loss of the latter to oligomerize independently (Fuchs and Hartmann, 2019). The resultant 20S proteasome is the most versatile member of the proteasome family. While Anbu is only found in bacteria, the proteasome is conserved in archaea and eukaryotes.
The HslV protease replaced the proteasome in most bacteria phyla, which probably evolved by gene duplication from the β-subunit precursor (Fuchs and Hartmann, 2019). The evolution of the proteasome might also become clear when comparing the modularity of the different proteases. The 20S proteasome can interact with different AAA+ unfoldases and non-ATP regulators, which bind to the top of the α-rings, such as the 19S regulatory particle or the PA200 (Fort et al., 2015; Pickering and Davies, 2012). The corresponding examples in archaea are the CDC48 and the ATP-independent PbaA/PbaB (Forouzan et al., 2012; Kusmierczyk et al., 2011). In bacteria are the unfoldase ring shaped complexes (ARC) and mycobacterial proteasomal ATPase (Mpa) known (Djuranovic et al., 2009). These regulators also form ring-shaped structures of different stoichiometries, which are somewhat comparable to the 19S regulatory particle in eukaryotic cells. Although not all are found in any given organism, they all share the same interaction and binding mode to the α-rings, which is the most conserved surface area on the whole 20S proteasome (Fuchs and Hartmann, 2019). Similarly, conserved areas are also found in the HslV protease of bacteria, although it has only one designated unfoldase binding partner, the HslU. This interaction partner is missing in Anbu and BPH, indicating that bacteria tended to evolve different proteases for different substrates, while the eukaryotic and archaeal strategy was to modulate their protease. This led to the development of different proteases in bacteria with specific targets for degradation, as for example the Lon protease degraded the isoE C-degron, while usually the ClpPX protease degrades unfolded proteins. In this context it seems logical, that the isoE C-degron would be degraded by HslUV. In contrast to that, our experiments showed no significant prolonged half-life of the tagged protein. As mentioned before, the HslV protease recognizes the charged amino acids serine and threonine. Since the bacteria phyla diverted its capacity of degradation into multiple

proteases, different proteases fulfil different tasks in degradation. A protease needs to be in charge of degrading proteins with hydrophobic amino acids at its C-terminus, which indicate a misfolded state. In this instance, the Lon protease is taking care of degradation of such proteins (Gur and Sauer, 2008).

Taken together, the proteasome evolved from a common precursor and the proteasome can be found in *archaea* and eukaryotic cells alike, while bacteria evolved many different proteases with different functions. While the mechanism of degradation for archaea and eukaryotic cells remains roughly the same, bacteria diverted their degradation capacity into different proteases. Thus, it becomes clear, why the proteasome is responsible for degradation of the isoE C-degron in eukaryotes, while in bacterial cells, the Lon-protease is responsible for the degradation.

6.1.3. Functions of unproductive splicing

Studies in the past mostly portrayed alternative splicing of pre-mRNAs as an event, which gives rise to proteins with altered function (Rambout et al., 2018). Indeed, different protein isoforms can have different effects on the regulation/signaling mechanism they are involved in. However, it is also known that alternative splicing often creates mRNA isoforms, which are unproductive in protein synthesis. One example for that are hnRNP D and hnRNP DL. Both mRNAs can contain a poison exon, which causes the RNA to be degraded by NMD (Kemmerer et al., 2018). Another example for an mRNA, which is degraded by NMD after alternative splicing is the mRNA coding for MAX isoform C (Kemmerer and Weigand, 2014). The mRNA of MAX isoform C includes a premature stop codon, which triggers NMD. In contrast to that, the mRNA of MAX isoform E escapes degradation by NMD, but instead codes for an extremely unstable protein.

Recently, other alternative splicing events leading to unstable proteins were found. mRNAs were the penultimate exon is skipped, escape NMD, which can lead to translation of the 3'-UTR. The subsequent addition of new amino acids to the alternative C-terminus of the encoded proteins, results in a general higher degradation rate (Preussner et al., 2020). A global analysis of all such generated, alternative C-termini revealed a general increase in the amino acids proline, leucine, serine and cysteine compared to the canonical C-terminus (Preussner et al., 2020). The amino acids cysteine and serine are known for oxidation, which subsequently induces protein degradation (Hamann et al., 2002). The most abundant motif in these C-termini was the PxxP motif, which suggests a higher intrinsic disorder (Kovacs et al., 2010). A higher intrinsic disorder is often correlated with reduced protein half-life (van der Lee et al., 2014). This suggests that the alternative splicing with skipping of the penultimate exon ultimately leads

to faster degradation and thus reduced protein function. We observed a similar mechanism with the alternative splicing of MAX isoform E, which likewise escapes NMD and creates a protein with highly reduced half-life (Peter et al., 2021). Alternative splicing coupled with rapid protein degradation could thus be part of a safety mechanism to prevent read-throughs and non-functional proteins.

However, in case of MAX isoform E, this unproductive, alternative splicing event is a programmed response to hypoxia (Kemmerer and Weigand, 2014). It could be that the resultant reduction of the MAX wild type protein causes a general decrease in energy uptake and a slowed proliferation rate, due to a reduced chance to bind MYC or MXD. Such general decrease in energy uptake will help the cell to survive under low oxygen conditions.

6.2. Aim 2: Analysis of AU-rich CDEs in the 3'-UTR of *UCP3*

6.2.1. Conformational flexibility of CDEs

Roquin has been reported to target RNA structures rather than linear sequence motifs (Leppek et al., 2013; Mino and Takeuchi, 2018; Schlundt et al., 2014; Tan et al., 2014). Thus, Roquin binding to its targets is affected by the folding probability of its cognate motifs. In the case of the two CDEs in the 3'-UTR of the *UCP3* mRNA, the two CDEs have different conformations in the absence of Roquin-1. While the first AU-pure CDE mainly samples a linear conformation as shown by CDE melting experiments, the second forms a CDE-like structure also in the absence of Roquin-1 (Binas et al., 2020). This indicates that the second CDE is more available for Roquin-1 binding, while the other might only be stably folded in the presence of Roquin-1 protein. This suggests that the second CDE is more preferred for Roquin binding. The AU-pure first CDE has a higher flexibility and a lower melting point than the second CDE (Binas et al., 2020). However, in the presence of the ROQ-domain, also the first SL is stably formed. This highlights the shape-specificity of Roquin for RNA structure, rather than a sequence requirement.

The binding capacity and mechanism of Roquin binding to the CDE structure is comparable to the binding mechanism to the *Tnf* CDE (Schlundt et al., 2014). Roquin-1 recognizes the *Tnf* CDE structure rather than the sequence identity, while the triloop motif, consisting of UGU nucleotides, supports the binding of the ROQ-domain. It also seems, that an adenine stretch at the 3' side of the stem, is increasing the binding affinity of ROQ to the *Tnf* SL (Schlundt et al., 2014). Since an adenine stretch is decreasing the helix melting temperature, it seems logical, that the *Tnf* CDE is not stably formed. Accordingly, it can only be detected in structural probing assays, when the CDE is stabilised by additional base pairs (Leppek et al., 2013). This seems similar to the ARE-like CDE in the *UCP3* 3'-UTR, which it is only formed in the presence

of Roquin-1. It also proofs that the *UCP3* SL structures are indeed CDEs, since they show the same binding mode as the *Tnf* CDE.

It has also been shown, that most CDEs have a low GC content and therefore are flexible structures (Leppek et al., 2013). A higher GC content also does not increase the Roquin affinity, which was shown extensively for the Roquin motifs in the *Ox40* 3'-UTR and also for the CDEs in *NFKBID* and *UCP3* (Braun et al., 2018; Leppek et al., 2013; Murakawa et al., 2015; Schaefer and Klein, 2016). This also indicates that a CDE structure can be formed *in vivo* inside the cell and is functional even when the folding probability is low. Thus, there might be many functional CDE or CDE-like structures, which are predicted to be unfolded or hidden inside bigger RNA structures to be more relevant. In the case of the RBP Roquin, a huge range of potential targets have been predicted by the algorithm Dynalign (Braun et al., 2018). Some of these targets were only active in specific cell lines, such as HEK 293 or HUVEC cells. This shows, that sequence motifs alone are an incomplete criteria for RNA structure prediction and conservation.

6.2.2. RBP competition for *cis*-elements

The classical example of the interaction between regulating RBPs and RNAs is the recognition of a linear consensus sequence by the RBP encoded by their target mRNA, often within the 3'-UTR (Li et al., 2017; Mino and Takeuchi, 2018). Most regulatory RBPs are known to interact with *cis*-elements in the 3'-UTR to stabilize or destabilize certain mRNAs (Shyu et al., 2008). Well studied examples of these *cis*-elements are the AREs and their *trans*-binding RBPs, such as AUF1 and the Human Antigen R (HuR). The basic ARE motif includes pentamers of AUUUA, nonamers of UUAUUUAUU and clusters composed of linked pentamers with/without nonamers (Wilusz et al., 2001). One example of an RBP binding to an AUUUA-pentamer is HuR (Hinman and Lou, 2008). It is an RBP, which is usually localised in the nucleus, but exposure to intrinsic or extrinsic stress signals causes a relocation to the cytoplasm, where HuR stabilizes target RNAs (Di Marco et al., 2005; Matsye et al., 2017). While HuR binding leads to mRA stabilization, most ARE-binding proteins initiate mRNA decay (Lal et al., 2004). Thus, mRNA abundance is determined by the competition between different RBPs for the same *cis*-element. An example for the competition between stabilizing and destabilizing factors is given by the mRNA of cyclin D1. This mRNA is bound in the nucleus by either HuR or AUF1, which compete for binding of the same mRNA element. Binding of HuR leads to mRNA stabilization and an increased translation rate, while the binding of AUF1 causes a decrease in mRNA and protein abundance through mRNA decay (Lal et al., 2004).

Another way to regulate the abundance of mRNAs is via microRNAs (miRNAs), which can bind to specific sequence motifs in the 3'-UTR of their target mRNAs (Bartel, 2009). miRNAs contain a complementary sequence consisting of 7mers or 8mers to their mRNA targets, resulting in the formation of a partially double-stranded RNA complex, which ultimately triggers degradation. miRNAs can also compete with RBPs for mRNA binding. One example is the competition between HuR and the miR-548c binding to the *TOP2A* (topoisomerase II alpha) mRNA. TOP2A is an enzyme, that relieves tension from supercoiled DNA. HuR is most abundant during the G2/M Phase of the cell cycle, which causes an increase in TOP2A. The topoisomerase is reduced by miR-548c, which binds to the 3'-UTR of the *TOP2A* mRNA and close to the recognition motif of HuR. When HuR binds to the *TOP2A* mRNA, the miRNA is unable to bind. Accordingly, overexpression of miR-548c caused a decrease in *TOP2A* mRNA and a reduced interaction of HuR with the mRNA (Srikantan et al., 2012).

Prior to this work, CDEs and AREs were thought to be separate *cis*-elements with complementary function in mRNA decay, which are recognised by different *trans*-acting factors. We recently were able to show, that AREs can also function as CDEs (Binas et al., 2020). Even more interesting, there seems to be a competition of binding between AUF1, which binds preferably linear AREs and the ROQ-domain of Roquin-1 (Binas et al., 2020). While the long adenine-rich stretch of CDE1 certainly provides the flexibility for the binding of the ROQ-domain, the stretch is also a binding motif for AUF1. This indicated that there might be a competition between AUF1 and Roquin-1 for binding of the same motif. Notably, the isoforms p37 and p45 of AUF1 are known to have a strong destabilizing effect on the mRNA they bind to (Loflin et al., 1999). These isoforms were also the top candidates, which bound the first SL of the *UCP3* mRNA in an RNA immunoprecipitation assay (Binas et al., 2020). This indicates that the first *UCP3* CDE is at the same time a functional ARE in its unfolded state and that the binding of AUF1 competes with Roquin-1 binding.

AUF1 has a binding affinity of around 300-800 nM for AREs, while Roquin-1 has with 100-400 nM a 2-3 times higher affinity for CDEs. Although the binding of Roquin is more affine, the binding affinity of AUF1 is in the same range. Indeed, NMR time scale experiments revealed, that both RBPs can bind the first *UCP3* CDE with similar affinity (Binas et al., 2020). AUF1 was able to unfold the first CDE and replace the ROQ-domain in the RNA complex. In consequence, *in vivo* the binding competition might simply depend on the availability of the corresponding RBP in the cell. The binding affinity favours the binding of Roquin to both SLs and AUF1 seems to be needed in excess in order to bind the unfolded ARE (Binas et al., 2020). It is worth mentioning, that the binding of AUF1 is strong enough that an excess of Roquin is needed to overcome AUF1 binding to the first SL of the 3'-UTR of *UCP3*. While Roquin and AUF1 perform the same task in mRNA destabilisation, AUF1 is further regulated by its paralog

hnRNP DL (Kemmerer et al., 2018). The RBP hnRNP DL regulates the expression of AUF1 by alternative splicing of a poison exon (Kemmerer et al., 2018). This indicates that the level of post-transcriptional regulation of *UCP3* is quite complex. The competition between Roquin and AUF1 binding could result in a tighter regulation of the *UCP3* mRNA. *UCP3* codes for an mitochondrial uncoupling protein, which transports protons across the mitochondrial membrane and is essential in the metabolism (Pohl et al., 2019). A higher synthesis of UCP3 protein could lead to a misbalance in the metabolism and proton balance of the cell. Since both are destabilising RBPs, the redundant targeting of the *UCP3* mRNA, might be a failsafe mechanism, to prevent excessive protein synthesis. It could be, that Roquin preferably binds to the *UCP3* 3'-UTR, but if Roquin is unavailable or reduced, AUF1 can likewise destabilize the mRNA accordingly. Further, the endonuclease Regnase-1 destabilises RNA and has nearly the same mode of recognition as does Roquin (Mino et al., 2015). Thus, Regnase-1 might be another factor destabilising the *UCP3* mRNA. This indicates a strong competition of destabilising factors in the case of the *UCP3* 3'-UTR.

6.3. Aim 3: Characterization of SARS-CoV-2 structural RNA elements

6.3.1. Functional RNA structures in the genome of SARS-CoV-2

As discussed above, RNA structure often includes function. Thus, targeting RNA structures to inhibit their function, is a viable strategy for drug design (Damase et al., 2021). In the first step to create functioning therapeutics against RNAs, you need to have an adequate knowledge of the RNA structure. Thus, in the process of understanding the RNA elements of SARS-CoV-2, we first performed comprehensive NMR and DMS footprinting experiments of the genomic regions important for viral replication and synthesis of viral proteins (Wacker et al., 2020). We were able to show, that 5_SL1 contains an open AU base pair flanking the upper helix of SL1, which is not resolved in most structural studies. This might provide a certain flexibility needed for Nsp1 recognition. Indeed, the structure and distance of 5_SL1 to the rest of the virus mRNA is important for translation (Lapointe et al., 2021; Shi et al., 2020). The Nsp1 protein recognizes the 5'-UTR SL1 for initiation of translation and a change in the distance of 5_SL1 to the 5'-Cap reduces the 5'-UTR mediated translation in the presence of Nsp1 (Lapointe et al., 2021).

Further, the stem of 5_SL5 showed high reactivity in the DMS footprinting experiments at the positions U288, U283, U297 and U267. While the NMR experiment was carried out at 10°C, the DMS footprinting experiment was performed at RT. When the according NMR experiment is performed under the same conditions as the DMS footprinting, the imino protons broaden at the exact same uridine residues as in the DMS footprinting experiment. These bases are usually paired with adenosine residues at 10°C while being unpaired at higher temperatures,

which highlights the importance of temperature on RNA structure (Wacker et al., 2020). This intrinsic flexibility might be important for efficient translation initiation, as the 5_SL5 stem contains the start codon of ORF1a. However, it might also be important for the other speculated functions of 5_SL5 in genome packaging or IRES-dependent translation (Masters, 2019; Slobodin et al., 2021).

An interesting target for inhibition is the SL2 located in the 3'-UTR. 3_SL2 folding is supposed to be important for the genome synthesis and replication of the virus (Chen et al., 2021; Goebel et al., 2004). The NMR and DMS analysis showed no stable base pairing interactions in the 13 nt large loop (Wacker et al., 2020). The residues inside the loop are flexible in an open conformation and tend not to base pair. This indicates a necessity for the 3_SL2 loop to stay open, likely for replication initiation. It was shown, that a switch between RNA structures in the 3'-UTR is involved in genome replication. The switching is formed between the base of 3_SL1 and the loop of 3_SL2 (Chen et al., 2021; Goebel et al., 2004; Madhugiri et al., 2016).

A similar role is known for the s2m motif in the 3'-UTR. The s2m motif is conserved across all β-CoVs and a mutation can lead to less pathogenic viruses (Chen et al., 2021; Gilbert and Tengs, 2021; Manfredonia et al., 2020). This highlights the importance of the s2m structure for viral replication. In comparison to SCoV1, the s2m motif of SCoV2 is bearing two mutations. One is at the lower helix and one destabilizes the pairing of the upper helix (Wacker et al., 2020). The s2m motif of SCoV2 is much more flexible, as indicated by NMR and DMS data. The change in the motif might be the reason for the increased spreading of SCoV2 compared to SCoV1. The s2m motif seems to be a potential target for drug design, since it is a strongly conserved and important structure for viral pathogenesis. It has been shown, that RNA viruses utilize some components of the host cells for their own benefit (Trobaugh et al., 2014). Indeed, the s2m motif of SARS-CoV-2 dimerizes with the miR 1307-3p. It is possible, that the dimerization of the s2m motif with the miR indirectly benefits the viral entry into cells near the already infected cell (Imperatore et al., 2021). This indicates, that the s2m motif might be a promising target for RNA drug admission.

Important structures with the coding part of the genome are the attenuator-hairpin and the pseudoknot. Since the exact control of viral protein ratios in the cell by ribosomal frameshifting is crucial for efficient replication of CoVs (Plant et al., 2010), these are also critical structures for drug design. Targeting these structures could potentially inhibit the viral replication and production of important viral proteins, such as Nsp12, the RNA-dependent RNA polymerase. The inhibition could lead to an accumulation of Nsp1 to Nsp10, while Nsp12 to Nsp16 are not translated, making the virus sterile due to treatment. This would improve the overall health of patients infected by SARS-CoV-2, while also giving a way for treatment of other viruses with a pseudoknot in between two ORFs. The role of a pseudoknot has been established in a huge

variety of RNA viruses, e.g. the *retroviridae* (such as HIV), *coronaviridae* (SARS-CoV-2), *totiviridae* (such as Leishmaniavirus) and *luteoviridae* (such as bean leafroll virus) family (Brierley et al., 2010, 2007; Cho et al., 2013; Giedroc et al., 2000). Having a drug inhibiting the pseudoknot function, several viral infections, such as HIV and Leishmaniavirus could be treated.

6.3.2. SARS-CoV-2 therapeutics

Most drugs to battle SARS-CoV-2 are designed to inhibit protein structures, such as the spike protein or Nsp12. The latter is inhibited by Remdesivir, which was the first drug approved by the FDA to treat patients suffering from SARS-CoV-2. Remdesivir was initially developed as an Ebola treatment, but a study on SARS-CoV-2 infected monkeys with Remdesivir revealed a significant reduction in viral load (Amirian and Levy, 2020; Williamson et al., 2020). It was shown, that it was especially useful in the treatment of coronaviruses (Amirian and Levy, 2020; Rezagholizadeh et al., 2021). Remdesivir is an inhibitor for the RdRp of SARS-CoV-2 and therefore blocks replication and transcription (Amirian and Levy, 2020; Rezagholizadeh et al., 2021). This drug is one of the very few medicaments, which allow a specific treatment of SARS-CoV-2. A downside of Remdesivir might be, that the virus could evolve to circumvent the effect. Indeed, there are reports of some SARS-CoV-2 variants, which are less sensitive to Remdesivir (Focosi et al., 2022; Szemiel et al., 2021). Although these strains are not spread far, it indicates a need for new drugs to treat patients infected by SARS-CoV-2. New drugs, which are currently in third clinical trial, generally intend to inhibit Nsp12, the RNA dependent RNA polymerase (RdRp) (Bertolin et al., 2021; Tian et al., 2021; Zhao et al., 2021).

Another strategy to treat SARS-CoV-2 infections is via the targeting of the spike protein. One strategy for example is the binding of antibodies to the spike protein. Antibodies targeting the Spike protein of SARS-CoV1 and 2 can effectively neutralise the virus and prevent viral entry (Gottlieb et al., 2021). The antibody therapy, consisting of bamlanivimab and etesevimab, reduced the viral load of patients at day 11 significantly compared to the placebo group (Gottlieb et al., 2021).

There are also some therapy targets, that prevent the virus from entering the cell through the angiotensin-converting enzyme 2 (ACE2). Antisense oligonucleotides (ASO) are a promising strategy to prevent the virus from entering cells. In last months, different approaches to prevent virus entry has been developed, e.g. aptamers against the ACE2-receptor, peptide-conjugated morpholino oligomers, ASOs or small chemical components (Li et al., 2021; Lulla et al., 2021; Rosenke et al., 2020; Song et al., 2020; Sreeramulu et al., 2021; Sun et al., 2021; Yang et al., 2021). The aptamers created have in common, that they bind portions of the spike protein and thereby prevent binding to the ACE2 receptor. If the receptor is blocked, the virus cannot enter

the cell (Emrani et al., 2021). The aptamers have a K_d value of 5.8 to 19.9 nM in binding to the spike protein receptor binding domain (Sun et al., 2021, 2021; Yang et al., 2021). Simulated modelling showed, that these aptamers have a similar binding capacity compared to the spike protein and thus compete with the binding to the ACE2 receptor. After some adaptations, the aptamer could be stored for 14 d at room temperature and could be used as an aerosol for infection prevention strategies (Sun et al., 2021). The IC_{50} value was reported to be at 0.42 nM (Sun et al., 2021). The aptamer could be used in a spray on a daily basis, if it proves to be non-toxic and well compatible with humans in clinical trials. The advantage of this method is, that aptamers can be produced easily and in high quantity.

While this is a prevention strategy, there are also approaches using ASOs for treatment of ill patients. The s2m motif is a conserved structure with a stable loop and a few exposed bases, which are present in astroviruses, some picornaviruses, noroviruses and certain coronaviruses (Jonassen et al., 1998; Rangan et al., 2020; Robertson et al., 2005; Tengs et al., 2013; Tengs and Jonassen, 2016). The high degree of conservation across species provides a promising target for antiviral drugs, especially since the mutational rate in this particular structure is relatively low. Consequently, a well-designed compound or ASO can make an efficient medicine to treat not only one, but a plethora of RNA viruses. Third generation ASOs contain locked nucleic acids, which provide high affinity base pairing to RNA and DNA (Hagedorn et al., 2018). Once base paired, the ASO then exhibits a sequence to recruit the RNase H. The RNase then cleaves the RNA in the RNA-DNA duplex leaving the ASO intact to bind to another target RNA. These locked nucleic acid ASOs (often called gapmers) have been successfully used in clinical trials to catalyse the degradation of target transcripts (Bonneau et al., 2019; Hagedorn et al., 2018). Lulla et al. designed gapmers against the s2m in the 3'-UTR of SARS-CoV-2 and astrovirus (Lulla et al., 2021). These gapmers showed in HeLa and A549 cells a reduction of GFP in the reporter assay and also reduced the replication of astrovirus in a cell-based reporter system, while also having low cytotoxic effects (Lulla et al., 2021). Another variant are the Peptide-conjugated morpholino oligomers (PPMO) used by Rosenke et al. (Rosenke et al., 2020). These oligomers showed sequence specific blockage of the 5'-UTR SL3, which contains the leader transcription regulatory sequence of SARS-CoV-2. In Vero-E6 cell culture these PPMOs showed a high reduction of viral titres of up to 4-6 log_{10}, indicating a high efficiency in reduction of viral replication (Rosenke et al., 2020). Another target to reduce the viral replication is SL1 in the 5'-UTR. Targeting this structure with ASOs reduces the amount of viral replication and is thus a possible treatment against SARS-CoV-2 (Vora et al., 2021).

Another idea to treat SARS-CoV-2 is the inhibition of structured elements, which are unlikely to change the structure due to mutations, with small molecules. In the attempt to find suitable

precursor for drug design to tackle this task, we screened for compounds binding to RNA structures of the SARS-CoV-2 genome and sorted them by their binding affinity and their target. Among the 15 screened RNAs, the pseudoknot and 3_SL3base RNA showed to be the most promising targets for a more refined drug design (Sreeramulu et al., 2021). The most promising binder was D01, which bound the pseudoknot and the s2m motif with a K_D of 6 µM. The frameshifting ability is vital for the virus, since already a small reduction causes a highly reduced infectivity (Plant et al., 2010). Another target, directly next to the pseudoknot, is the att-hairpin of the FSE as shown by Haniff et al. (Haniff et al., 2020). They screened and designed a small chemical compound binding the att-hairpin of the FSE. Once the binder proved to efficiently bind the viral RNA, the binder was modified to recruit a ribonuclease to destroy the viral genome. They were able to show, that the stabilisation of the FSE leads to a reduced frameshifting ability *in vitro*. A combination of targeting the att-hairpin, pseudoknot and s2m motif might lead to a very potent drug against viruses containing an FSE, while also inhibiting the reproduction of many different viruses. Thus, it might provide a specific broad-spectrum therapy option. In addition, many viruses, such as HIV or SARS-CoV-2, contain conserved RNA elements, which can be targeted by RNA drugs. Thus, RNA drugs are a promising field for treatment options of a plethora of illnesses.

6.4. Outlook

6.4.1. Aim 1: Characterization of the coupling between pre-mRNA splicing and protein degradation

So far, I was able to determine the exact amino acids necessary for fast and rapid degradation in bacteria, yeast and mammalian cells. The degradation mechanism relies on hydrophobic amino acids and is likely to be a part of a stress response. While the proteasome is responsible for the degradation in mammalian cells, the Lon protease is degrading tagged proteins in *E. coli*. Due to its efficiency and universal applicability, the isoE C-degron could be used as tool in Synthetic Biology for programmed protein degradation in reporter assays. The degron could be fused via a cleavable linker to a reporter protein, which is constantly degraded. After cleaving the linker and thus the degron, the reporter protein is stabilized and can be detected. This might be applicable for enzyme kinetic studies. The protein of interest might be degraded until cleavage of the linker containing the degron is performed. After cleavage, the reporter system is “switched on” and function or enzyme kinetic can be measured in a precise and efficient manner.

6.4.2. Aim 2: Analysis of AU-rich CDEs in the 3’-UTR of *UCP3*

We were able to identify a previously unknown binding mechanism for the RBP Roquin-1. Roquin-1 can bind structured SLs, which can be AU-rich CDEs with high affinity and competes with AUF1 for binding *in vitro*. In a next step, competition for CDEs between these two proteins and eventually also further RBPs, like HuR and Regnase-1, should be shown in cells. Further, this finding generally indicates that conserved structures might be more relevant than sequence identity for regulatory elements. It also indicates that there is a need for scanning of conserved structures across species (Braun et al., 2018). In order to find more regulatory active structures in mammalian cells, a high-throughput screening might be the answer. The screening system could be based on a dual fluorescence system, where one fluorophore carries a multiple cloning site in the 3’-UTR for insertion of a randomised pool. The transfected cells should also be grown under different conditions, to see, if some regulatory elements are only active under stress conditions, e.g. hypoxia. In a second analysis step, the responsible RBP could be determined using an immunoprecipitation assay.

6.5. Aim 3: Characterization of SARS-CoV-2 structural RNA elements

In the studies performed by us, we could determine the structure and general druggability of functional RNA elements of the SARS-CoV-2 genome with potential for drug development. The screening with small chemical compounds in order to find suitable RNA binder, gave us a first RNA binder with good affinity of binding the pseudoknot and the s2m motif. This binder could be a potential precursor for a drug, which is effective against SARS-CoV-2 and other

RNA viruses with a pseudoknot containing FSE similar to the one in SARS-CoV-2. Since these studies have been performed *in vitro*, advanced studies *in vivo* and in animal models have to be done. The compound could have a cytotoxic effect in cells and should be tested for its permeability of the cell membrane. In order to do so, a fluorescence- or chemiluminescence-based reporter assay could be used. Indeed, such assays have been developed and used to test for potential drugs (Bhatt et al., 2021; Zhao et al., 2021). After modifying the binder to be more permeable or less toxic for the cells, the binder could be linked with another potential binder inhibiting another part of the virus genome in close proximity, to make it more effective in treating the virus. The optimised binder could then be used in 3D cell culture to mimic in a simplified way the effect on cell clusters. A more complex cell culture system including two or three different, but synergetic cell lines, could mimic a simplified organ and the effect of the drug precursor on the mixture of cells. In a long run, the binder could be developed to pose an effective drug.

7. References

Acosta, J.C., Ferrándiz, N., Bretones, G., Torrano, V., Blanco, R., Richard, C., O'Connell, B., Sedivy, J., Delgado, M.D., León, J., 2008. Myc Inhibits p27-Induced Erythroid Differentiation of Leukemia Cells by Repressing Erythroid Master Genes without Reversing p27-Mediated Cell Cycle Arrest. Mol. Cell. Biol. 28, 7286–7295. https://doi.org/10.1128/MCB.00752-08

Allevato, M., Bolotin, E., Grossman, M., Mane-Padros, D., Sladek, F.M., Martinez, E., 2017. Sequence-specific DNA binding by MYC/MAX to low-affinity non-E-box motifs. PLoS ONE 12. https://doi.org/10.1371/journal.pone.0180147

Amirian, E.S., Levy, J.K., 2020. Current knowledge about the antivirals remdesivir (GS-5734) and GS-441524 as therapeutic options for coronaviruses. One Health 9, 100128. https://doi.org/10.1016/j.onehlt.2020.100128

Arribere, J.A., Fire, A.Z., n.d. Nonsense mRNA suppression via nonstop decay. eLife 7. https://doi.org/10.7554/eLife.33292

Ayer, D.E., Eisenman, R.N., 1993. A switch from Myc:Max to Mad:Max heterocomplexes accompanies monocyte/macrophage differentiation. Genes Dev. 7, 2110–2119. https://doi.org/10.1101/gad.7.11.2110

Ayer, D.E., Kretzner, L., Eisenman, R.N., 1993. Mad: A heterodimeric partner for Max that antagonizes Myc transcriptional activity. Cell 72, 211–222. https://doi.org/10.1016/0092-8674(93)90661-9

Baker, T.A., Sauer, R.T., 2012. ClpXP, an ATP-powered unfolding and protein-degradation machine. Biochim. Biophys. Acta BBA - Mol. Cell Res. 1823, 15–28. https://doi.org/10.1016/j.bbamcr.2011.06.007

Balchin, D., Hayer-Hartl, M., Hartl, F.U., 2016. In vivo aspects of protein folding and quality control. Science 353, aac4354. https://doi.org/10.1126/science.aac4354

Bard, J.A.M., Goodall, E.A., Greene, E.R., Jonsson, E., Dong, K.C., Martin, A., 2018. Structure and Function of the 26S Proteasome. Annu. Rev. Biochem. 87, 697–724. https://doi.org/10.1146/annurev-biochem-062917-011931

Bartel, D.P., 2009. MicroRNA Target Recognition and Regulatory Functions. Cell 136, 215–233. https://doi.org/10.1016/j.cell.2009.01.002

Ben-Nissan, G., Sharon, M., 2014. Regulating the 20S Proteasome Ubiquitin-Independent Degradation Pathway. Biomolecules 4, 862–884. https://doi.org/10.3390/biom4030862

Berberich, S.J., Cole, M.D., 1992. Casein kinase II inhibits the DNA-binding activity of Max homodimers but not Myc/Max heterodimers. Genes Dev. 6, 166–176. https://doi.org/10.1101/gad.6.2.166

Berenguer, J., Herrera, A., Vuolo, L., Torroba, B., Llorens, F., Sumoy, L., Pons, S., 2013. MicroRNA 22 regulates cell cycle length in cerebellar granular neuron precursors. Mol. Cell. Biol. 33, 2706–2717. https://doi.org/10.1128/MCB.00338-13

Bertolin, A.P., Weissmann, F., Zeng, J., Posse, V., Milligan, J.C., Canal, B., Ulferts, R., Wu, M., Drury, L.S., Howell, M., Beale, R., Diffley, J.F.X., 2021. Identifying SARS-CoV-2 antiviral compounds by screening for small molecule inhibitors of nsp12/7/8 RNA-dependent RNA polymerase. Biochem. J. 478, 2425–2443. https://doi.org/10.1042/BCJ20210200

Bhatt, P.R., Scaiola, A., Loughran, G., Leibundgut, M., Kratzel, A., Meurs, R., Dreos, R., O'Connor, K.M., McMillan, A., Bode, J.W., Thiel, V., Gatfield, D., Atkins, J.F., Ban, N., 2021. Structural basis of ribosomal frameshifting during translation of the SARS-CoV-2 RNA genome. Science 372, 1306–1313. https://doi.org/10.1126/science.abf3546

Binas, O., Tants, J.-N., Peter, S.A., Janowski, R., Davydova, E., Braun, J., Niessing, D., Schwalbe, H., Weigand, J.E., Schlundt, A., 2020. Structural basis for the recognition of transiently structured AU-rich elements by Roquin. Nucleic Acids Res. 48, 7385–7403. https://doi.org/10.1093/nar/gkaa465

Blackwood, E.M., Lüscher, B., Eisenman, R.N., 1992. Myc and Max associate in vivo. Genes Dev. 6, 71–80. https://doi.org/10.1101/gad.6.1.71

Bochtler, M., Ditzel, L., Groll, M., Hartmann, C., Huber, R., 1999. The proteasome. Annu. Rev. Biophys. Biomol. Struct. 28, 295–317. https://doi.org/10.1146/annurev.biophys.28.1.295

Bonneau, E., Neveu, B., Kostantin, E., Tsongalis, G.J., De Guire, V., 2019. How close are miRNAs from clinical practice? A perspective on the diagnostic and therapeutic market. EJIFCC 30, 114–127.

Braun, J., Fischer, S., Xu, Z.Z., Sun, H., Ghoneim, D.H., Gimbel, A.T., Plessmann, U., Urlaub, H., Mathews, D.H., Weigand, J.E., 2018. Identification of new high affinity targets for Roquin based on structural conservation. Nucleic Acids Res. 46, 12109–12125. https://doi.org/10.1093/nar/gky908

Braunstein, I., Zach, L., Allan, S., Kalies, K.-U., Stanhill, A., 2015. Proteasomal degradation of preemptive quality control (pQC) substrates is mediated by an AIRAPL–p97 complex. Mol. Biol. Cell 26, 3719–3727. https://doi.org/10.1091/mbc.E15-02-0085

Brierley, I., Gilbert, R.J.C., Pennell, S., 2010. Pseudoknot-Dependent Programmed —1 Ribosomal Frameshifting: Structures, Mechanisms and Models, in: Atkins, J.F., Gesteland, R.F. (Eds.), Recoding: Expansion of Decoding Rules Enriches Gene Expression, Nucleic Acids and Molecular Biology. Springer, New York, NY, pp. 149–174. https://doi.org/10.1007/978-0-387-89382-2_7

Brierley, I., Pennell, S., Gilbert, R.J.C., 2007. Viral RNA pseudoknots: versatile motifs in gene expression and replication. Nat. Rev. Microbiol. 5, 598–610. https://doi.org/10.1038/nrmicro1704

Carey, K.T., Wickramasinghe, V.O., 2018. Regulatory Potential of the RNA Processing Machinery: Implications for Human Disease. Trends Genet. TIG 34, 279–290. https://doi.org/10.1016/j.tig.2017.12.012

Carroll, V.A., Ashcroft, M., 2005. Targeting the molecular basis for tumour hypoxia. Expert Rev. Mol. Med. 7, 1–16. https://doi.org/10.1017/S1462399405009117

Cascón, A., Robledo, M., 2012. MAX and MYC: A Heritable Breakup. Cancer Res. 72, 3119–3124. https://doi.org/10.1158/0008-5472.CAN-11-3891

Castell, A., Yan, Q., Fawkner, K., Hydbring, P., Zhang, F., Verschut, V., Franco, M., Zakaria, S.M., Bazzar, W., Goodwin, J., Zinzalla, G., Larsson, L.-G., 2018. A selective high affinity MYC-binding compound inhibits MYC:MAX interaction and MYC-dependent tumor cell proliferation. Sci. Rep. 8, 10064. https://doi.org/10.1038/s41598-018-28107-4

Chang, Y.-F., Imam, J.S., Wilkinson, M.F., 2007. The nonsense-mediated decay RNA surveillance pathway. Annu. Rev. Biochem. 76, 51–74. https://doi.org/10.1146/annurev.biochem.76.050106.093909

Chee, N.T., Lohse, I., Brothers, S.P., 2019. mRNA-to-protein translation in hypoxia. Mol. Cancer 18, 49. https://doi.org/10.1186/s12943-019-0968-4

Chen, M., Manley, J.L., 2009. Mechanisms of alternative splicing regulation: insights from molecular and genomics approaches. Nat. Rev. Mol. Cell Biol. 10, 741–754. https://doi.org/10.1038/nrm2777

Chen, S.-C., Olsthoorn, R.C.L., 2010. Group-specific structural features of the 5′-proximal sequences of coronavirus genomic RNAs. Virology 401, 29–41. https://doi.org/10.1016/j.virol.2010.02.007

Chen, S.-C., Olsthoorn, R.C.L., Yu, C.-H., 2021. Structural phylogenetic analysis reveals lineage-specific RNA repetitive structural motifs in all coronaviruses and associated variations in SARS-CoV-2. Virus Evol. 7, veab021. https://doi.org/10.1093/ve/veab021

Cho, C.-P., Lin, S.-C., Chou, M.-Y., Hsu, H.-T., Chang, K.-Y., 2013. Regulation of Programmed Ribosomal Frameshifting by Co-Translational Refolding RNA Hairpins. PLoS ONE 8, e62283. https://doi.org/10.1371/journal.pone.0062283

Choudhury, R., 2018. Hypoxia and hyperbaric oxygen therapy: a review. Int. J. Gen. Med. 11, 431–442. https://doi.org/10.2147/IJGM.S172460

Cieply, B., Carstens, R.P., 2015. Functional roles of alternative splicing factors in human disease. WIREs RNA 6, 311–326. https://doi.org/10.1002/wrna.1276

Čivljak, R., Markotić, A., Kuzman, I., 2020. The third coronavirus epidemic in the third millennium: what's next? Croat. Med. J. 61, 1–4. https://doi.org/10.3325/cmj.2020.61.1

Cui, J., Li, F., Shi, Z.-L., 2019. Origin and evolution of pathogenic coronaviruses. Nat. Rev. Microbiol. 17, 181–192. https://doi.org/10.1038/s41579-018-0118-9

Cui, X.-G., Han, Z.-T., He, S.-H., Wu, X., Chen, T.-R., Shao, C.-H., Chen, D.-L., Su, N., Chen, Y.-M., Wang, T., Wang, J., Song, D.-W., Yan, W.-J., Yang, X.-H., Liu, T., Wei, H.-F., Xiao, J., 2017. HIF1/2α mediates hypoxia-induced LDHA expression in human pancreatic cancer cells. Oncotarget 8, 24840–24852. https://doi.org/10.18632/oncotarget.15266

Damase, T.R., Sukhovershin, R., Boada, C., Taraballi, F., Pettigrew, R.I., Cooke, J.P., 2021. The Limitless Future of RNA Therapeutics. Front. Bioeng. Biotechnol. 9, 628137. https://doi.org/10.3389/fbioe.2021.628137

Das, A., Ahmed, R., Akhtar, S., Begum, K., Banu, S., 2021. An overview of basic molecular biology of SARS-CoV-2 and current COVID-19 prevention strategies. Gene Rep. 23, 101122. https://doi.org/10.1016/j.genrep.2021.101122

Davies, K.J.A., 2001. Degradation of oxidized proteins by the 20S proteasome. Biochimie 83, 301–310. https://doi.org/10.1016/S0300-9084(01)01250-0

De Conti, L., Baralle, M., Buratti, E., 2013. Exon and intron definition in pre-mRNA splicing. Wiley Interdiscip. Rev. RNA 4, 49–60. https://doi.org/10.1002/wrna.1140

De Mot, R., 2007. Actinomycete-like proteasomes in a Gram-negative bacterium. Trends Microbiol. 15, 335–338. https://doi.org/10.1016/j.tim.2007.06.002

Deckert, J., Hartmuth, K., Boehringer, D., Behzadnia, N., Will, C.L., Kastner, B., Stark, H., Urlaub, H., Lührmann, R., 2006. Protein Composition and Electron Microscopy Structure of Affinity-Purified Human Spliceosomal B Complexes Isolated under Physiological Conditions. Mol. Cell. Biol. 26, 5528–5543. https://doi.org/10.1128/MCB.00582-06

Deshaies, R.J., Joazeiro, C.A.P., 2009. RING domain E3 ubiquitin ligases. Annu. Rev. Biochem. 78, 399–434. https://doi.org/10.1146/annurev.biochem.78.101807.093809

Di Marco, S., Mazroui, R., Dallaire, P., Chittur, S., Tenenbaum, S.A., Radzioch, D., Marette, A., Gallouzi, I.-E., 2005. NF-kappa B-mediated MyoD decay during muscle wasting requires nitric oxide synthase mRNA stabilization, HuR protein, and nitric oxide release. Mol. Cell. Biol. 25, 6533–6545. https://doi.org/10.1128/MCB.25.15.6533-6545.2005

Diolaiti, D., McFerrin, L., Carroll, P., Eisenman, R.N., 2015. Functional Interactions Among Members of the MAX and MLX Transcriptional Network During Oncogenesis. Biochim. Biophys. Acta 1849, 484–500. https://doi.org/10.1016/j.bbagrm.2014.05.016

Dissmeyer, N., Rivas, S., Graciet, E., 2018. Life and death of proteins after protease cleavage: protein degradation by the N-end rule pathway. New Phytol. 218, 929–935. https://doi.org/10.1111/nph.14619

Djuranovic, S., Hartmann, M.D., Habeck, M., Ursinus, A., Zwickl, P., Martin, J., Lupas, A.N., Zeth, K., 2009. Structure and activity of the N-terminal substrate recognition domains in proteasomal ATPases. Mol. Cell 34, 580–590. https://doi.org/10.1016/j.molcel.2009.04.030

Dominguez, D., Freese, P., Alexis, M.S., Su, A., Hochman, M., Palden, T., Bazile, C., Lambert, N.J., Van Nostrand, E.L., Pratt, G.A., Yeo, G.W., Graveley, B.R., Burge, C.B., 2018. Sequence, Structure, and Context Preferences of Human RNA Binding Proteins. Mol. Cell 70, 854-867.e9. https://doi.org/10.1016/j.molcel.2018.05.001

Dong, Y., Zhang, S., Wu, Z., Li, X., Wang, W.L., Zhu, Y., Stoilova-McPhie, S., Lu, Y., Finley, D., Mao, Y., 2019. Cryo-EM structures and dynamics of substrate-engaged human 26S proteasome. Nature 565, 49–55. https://doi.org/10.1038/s41586-018-0736-4

Dougan, D.A., Micevski, D., Truscott, K.N., 2012. The N-end rule pathway: from recognition by N-recognins, to destruction by AAA+proteases. Biochim. Biophys. Acta 1823, 83–91. https://doi.org/10.1016/j.bbamcr.2011.07.002

Dunwoodie, S.L., 2009. The role of hypoxia in development of the Mammalian embryo. Dev. Cell 17, 755–773. https://doi.org/10.1016/j.devcel.2009.11.008

Dyle, M.C., Kolakada, D., Cortazar, M.A., Jagannathan, S., 2020. How to get away with nonsense: Mechanisms and consequences of escape from nonsense-mediated RNA decay. WIREs RNA 11, e1560. https://doi.org/10.1002/wrna.1560

Emrani, J., Ahmed, M., Jeffers-Francis, L., Teleha, J.C., Mowa, N., Newman, R.H., Thomas, M.D., 2021. SARS-COV-2, infection, transmission, transcription, translation, proteins, and treatment: A review. Int. J. Biol. Macromol. 193, 1249–1273. https://doi.org/10.1016/j.ijbiomac.2021.10.172

Essig, K., Kronbeck, N., Guimaraes, J.C., Lohs, C., Schlundt, A., Hoffmann, A., Behrens, G., Brenner, S., Kowalska, J., Lopez-Rodriguez, C., Jemielity, J., Holtmann, H., Reiche, K., Hackermüller, J., Sattler, M., Zavolan, M., Heissmeyer, V., 2018. Roquin targets mRNAs in a 3′-UTR-specific manner by different modes of regulation. Nat. Commun. 9, 3810. https://doi.org/10.1038/s41467-018-06184-3

Farina, A.R., Cappabianca, L., Sebastiano, M., Zelli, V., Guadagni, S., Mackay, A.R., 2020. Hypoxia-induced alternative splicing: the 11th Hallmark of Cancer. J. Exp. Clin. Cancer Res. CR 39. https://doi.org/10.1186/s13046-020-01616-9

Filichkin, S., Priest, H.D., Megraw, M., Mockler, T.C., 2015. Alternative splicing in plants: directing traffic at the crossroads of adaptation and environmental stress. Curr. Opin. Plant Biol. 24, 125–135. https://doi.org/10.1016/j.pbi.2015.02.008

Fischer, S., Liddo, A.D., Taylor, K., Gerhardus, J.S., Sobczak, K., Zarnack, K., Weigand, J.E., 2020. Muscleblind-like 2 controls the hypoxia response of cancer cells. RNA 26, 648–663. https://doi.org/10.1261/rna.073353.119

Focosi, D., Maggi, F., McConnell, S., Casadevall, A., 2022. Very low levels of remdesivir resistance in SARS-COV-2 genomes after 18 months of massive usage during the COVID19 pandemic: A GISAID exploratory analysis. Antiviral Res. 198, 105247. https://doi.org/10.1016/j.antiviral.2022.105247

Forouzan, D., Ammelburg, M., Hobel, C.F., Ströh, L.J., Sessler, N., Martin, J., Lupas, A.N., 2012. The Archaeal Proteasome Is Regulated by a Network of AAA ATPases. J. Biol. Chem. 287, 39254–39262. https://doi.org/10.1074/jbc.M112.386458

Fort, P., Kajava, A.V., Delsuc, F., Coux, O., 2015. Evolution of proteasome regulators in eukaryotes. Genome Biol. Evol. 7, 1363–1379. https://doi.org/10.1093/gbe/evv068

Fox-Walsh, K.L., Dou, Y., Lam, B.J., Hung, S.-P., Baldi, P.F., Hertel, K.J., 2005. The architecture of pre-mRNAs affects mechanisms of splice-site pairing. Proc. Natl. Acad. Sci. U. S. A. 102, 16176–16181. https://doi.org/10.1073/pnas.0508489102

Fraisl, P., Mazzone, M., Schmidt, T., Carmeliet, P., 2009. Regulation of angiogenesis by oxygen and metabolism. Dev. Cell 16, 167–179. https://doi.org/10.1016/j.devcel.2009.01.003

Fuchs, A.C.D., Alva, V., Maldoner, L., Albrecht, R., Hartmann, M.D., Martin, J., 2017. The Architecture of the Anbu Complex Reflects an Evolutionary Intermediate at the Origin of the Proteasome System. Struct. Lond. Engl. 1993 25, 834-845.e5. https://doi.org/10.1016/j.str.2017.04.005

Fuchs, A.C.D., Hartmann, M.D., 2019. On the Origins of Symmetry and Modularity in the Proteasome Family. BioEssays 41, 1800237. https://doi.org/10.1002/bies.201800237

Führer, F., Müller, A., Baumann, H., Langklotz, S., Kutscher, B., Narberhaus, F., 2007. Sequence and Length Recognition of the C-terminal Turnover Element of LpxC, a Soluble Substrate of the Membrane-bound FtsH Protease. J. Mol. Biol. 372, 485–496. https://doi.org/10.1016/j.jmb.2007.06.083

Gallego-Paez, L.M., Bordone, M.C., Leote, A.C., Saraiva-Agostinho, N., Ascensão-Ferreira, M., Barbosa-Morais, N.L., 2017. Alternative splicing: the pledge, the turn, and the prestige. Hum. Genet. 136, 1015–1042. https://doi.org/10.1007/s00439-017-1790-y

Geiler-Samerotte, K.A., Dion, M.F., Budnik, B.A., Wang, S.M., Hartl, D.L., Drummond, D.A., 2011. Misfolded proteins impose a dosage-dependent fitness cost and trigger a cytosolic unfolded protein response in yeast. Proc. Natl. Acad. Sci. U. S. A. 108, 680–685. https://doi.org/10.1073/pnas.1017570108

Geuens, T., Bouhy, D., Timmerman, V., 2016. The hnRNP family: insights into their role in health and disease. Hum. Genet. 135, 851–867. https://doi.org/10.1007/s00439-016-1683-5

Giedroc, D.P., Theimer, C.A., Nixon, P.L., 2000. Structure, stability and function of RNA pseudoknots involved in stimulating ribosomal frameshifting. J. Mol. Biol. 298, 167–185. https://doi.org/10.1006/jmbi.2000.3668

Gilbert, C., Tengs, T., 2021. No species-level losses of s2m suggests critical role in replication of SARS-related coronaviruses. Sci. Rep. 11, 16145. https://doi.org/10.1038/s41598-021-95496-4

Glisovic, T., Bachorik, J.L., Yong, J., Dreyfuss, G., 2008. RNA-binding proteins and post-transcriptional gene regulation. FEBS Lett. 582, 1977–1986. https://doi.org/10.1016/j.febslet.2008.03.004

Goebel, S.J., Hsue, B., Dombrowski, T.F., Masters, P.S., 2004. Characterization of the RNA components of a putative molecular switch in the 3' untranslated region of the murine coronavirus genome. J. Virol. 78, 669–682. https://doi.org/10.1128/jvi.78.2.669-682.2004

Gonzales, M., Frank, E., Levine, A., Woodgate, R., 1998. Lon-mediated proteolysis of the Escherichia coli UmuD mutagenesis protein: in vitro degradation and identification of residues required for proteolysis [WWW Document]. Genes Dev. https://doi.org/10.1101/gad.12.24.3889

Gottlieb, R.L., Nirula, A., Chen, P., Boscia, J., Heller, B., Morris, J., Huhn, G., Cardona, J., Mocherla, B., Stosor, V., Shawa, I., Kumar, P., Adams, A.C., Van Naarden, J., Custer, K.L., Durante, M., Oakley, G., Schade, A.E., Holzer, T.R., Ebert, P.J., Higgs, R.E., Kallewaard, N.L., Sabo, J., Patel, D.R., Klekotka, P., Shen, L., Skovronsky, D.M., 2021. Effect of Bamlanivimab as Monotherapy or in Combination With Etesevimab on Viral Load in Patients With Mild to Moderate COVID-19. JAMA 325, 632–644. https://doi.org/10.1001/jama.2021.0202

Grandori, C., Cowley, S.M., James, L.P., Eisenman, R.N., 2000. The Myc/Max/Mad Network and the Transcriptional Control of Cell Behavior. Annu. Rev. Cell Dev. Biol. 16, 653–699. https://doi.org/10.1146/annurev.cellbio.16.1.653

Graveley, B.R., 2001. Alternative splicing: increasing diversity in the proteomic world. Trends Genet. TIG 17, 100–107. https://doi.org/10.1016/s0168-9525(00)02176-4

Graveley, B.R., 2000. Sorting out the complexity of SR protein functions. RNA 6, 1197–1211.

Gur, E., Sauer, R.T., 2009. Degrons in protein substrates program the speed and operating efficiency of the AAA+ Lon proteolytic machine. Proc. Natl. Acad. Sci. 106, 18503–18508. https://doi.org/10.1073/pnas.0910392106

Gur, E., Sauer, R.T., 2008. Recognition of misfolded proteins by Lon, a AAA(+) protease. Genes Dev. 22, 2267–2277. https://doi.org/10.1101/gad.1670908

Gur, E., Vishkautzan, M., Sauer, R.T., 2012. Protein unfolding and degradation by the AAA+ Lon protease: Lon Can Operate as a Powerful Protein Unfoldase. Protein Sci. 21, 268–278. https://doi.org/10.1002/pro.2013

Haase, V.H., 2013. Regulation of erythropoiesis by hypoxia-inducible factors. Blood Rev. 27, 41–53. https://doi.org/10.1016/j.blre.2012.12.003

Hagedorn, P.H., Persson, R., Funder, E.D., Albæk, N., Diemer, S.L., Hansen, D.J., Møller, M.R., Papargyri, N., Christiansen, H., Hansen, B.R., Hansen, H.F., Jensen, M.A., Koch, T., 2018. Locked nucleic acid: modality, diversity, and drug discovery. Drug Discov. Today 23, 101–114. https://doi.org/10.1016/j.drudis.2017.09.018

Hamann, M., Zhang, T., Hendrich, S., Thomas, J.A., 2002. [15] Quantitation of protein sulfinic and sulfonic acid, irreversibly oxidized protein cysteine sites in cellular proteins, in: Sies, H., Packer, L. (Eds.), Methods in Enzymology, Protein Sensors and Reactive Oxygen Species - Part B: Thiol Enzymes and Proteins. Academic Press, pp. 146–156. https://doi.org/10.1016/S0076-6879(02)48634-X

Haniff, H.S., Tong, Y., Liu, X., Chen, J.L., Suresh, B.M., Andrews, R.J., Peterson, J.M., O'Leary, C.A., Benhamou, R.I., Moss, W.N., Disney, M.D., 2020. Targeting the SARS-CoV-2 RNA Genome with

Small Molecule Binders and Ribonuclease Targeting Chimera (RIBOTAC) Degraders. ACS Cent. Sci. 6, 1713–1721. https://doi.org/10.1021/acscentsci.0c00984

Hernández-Elvira, M., Torres-Quiroz, F., Escamilla-Ayala, A., Domínguez-Martin, E., Escalante, R., Kawasaki, L., Ongay-Larios, L., Coria, R., 2018. The Unfolded Protein Response Pathway in the Yeast Kluyveromyces lactis. A Comparative View among Yeast Species. Cells 7, 106. https://doi.org/10.3390/cells7080106

Hiller, M.M., Finger, A., Schweiger, M., Wolf, D.H., 1996. ER degradation of a misfolded luminal protein by the cytosolic ubiquitin-proteasome pathway. Science 273, 1725–1728. https://doi.org/10.1126/science.273.5282.1725

Hinman, M.N., Lou, H., 2008. Diverse molecular functions of Hu proteins. Cell. Mol. Life Sci. CMLS 65, 3168–3181. https://doi.org/10.1007/s00018-008-8252-6

Hishida, T., Nozaki, Y., Nakachi, Y., Mizuno, Y., Okazaki, Y., Ema, M., Takahashi, S., Nishimoto, M., Okuda, A., 2011. Indefinite self-renewal of ESCs through Myc/Max transcriptional complex-independent mechanisms. Cell Stem Cell 9, 37–49. https://doi.org/10.1016/j.stem.2011.04.020

Hochstrasser, M., 1995. Ubiquitin, proteasomes, and the regulation of intracellular protein degradation. Curr. Opin. Cell Biol. 7, 215–223. https://doi.org/10.1016/0955-0674(95)80031-X

Höckel, M., Vaupel, P., 2001. Tumor Hypoxia: Definitions and Current Clinical, Biologic, and Molecular Aspects. JNCI J. Natl. Cancer Inst. 93, 266–276. https://doi.org/10.1093/jnci/93.4.266

Holmquist-Mengelbier, L., Fredlund, E., Löfstedt, T., Noguera, R., Navarro, S., Nilsson, H., Pietras, A., Vallon-Christersson, J., Borg, A., Gradin, K., Poellinger, L., Påhlman, S., 2006. Recruitment of HIF-1alpha and HIF-2alpha to common target genes is differentially regulated in neuroblastoma: HIF-2alpha promotes an aggressive phenotype. Cancer Cell 10, 413–423. https://doi.org/10.1016/j.ccr.2006.08.026

Hurlin, P.J., Ayer, D.E., Grandori, C., Eisenman, R.N., 1994. The Max Transcription Factor Network: Involvement of Mad in Differentiation and an Approach to Identification of Target Genes. Cold Spring Harb. Symp. Quant. Biol. 59, 109–116. https://doi.org/10.1101/SQB.1994.059.01.014

Huston, N.C., Wan, H., de Cesaris Araujo Tavares, R., Wilen, C., Pyle, A.M., 2020. Comprehensive in-vivo secondary structure of the SARS-CoV-2 genome reveals novel regulatory motifs and mechanisms. bioRxiv 2020.07.10.197079. https://doi.org/10.1101/2020.07.10.197079

Imperatore, J.A., Cunningham, C.L., Pellegrene, K.A., Brinson, R.G., Marino, J.P., Evanseck, J.D., Mihailescu, M.R., 2021. Highly conserved s2m element of SARS-CoV-2 dimerizes via a kissing complex and interacts with host miRNA-1307-3p. Nucleic Acids Res. 50, 1017–1032. https://doi.org/10.1093/nar/gkab1226

Inobe, T., Fishbain, S., Prakash, S., Matouschek, A., 2011. Defining the geometry of the two-component proteasome degron. Nat. Chem. Biol. 7, 161–167. https://doi.org/10.1038/nchembio.521

Janowski, R., Heinz, G.A., Schlundt, A., Wommelsdorf, N., Brenner, S., Gruber, A.R., Blank, M., Buch, T., Buhmann, R., Zavolan, M., Niessing, D., Heissmeyer, V., Sattler, M., 2016. Roquin recognizes a non-canonical hexaloop structure in the 3'-UTR of Ox40. Nat. Commun. 7, 11032. https://doi.org/10.1038/ncomms11032

Jastrab, J.B., Darwin, K.H., 2015. Bacterial Proteasomes. Annu. Rev. Microbiol. 69, 109–127. https://doi.org/10.1146/annurev-micro-091014-104201

Jonassen, C.M., Jonassen, T.O., Grinde, B., 1998. A common RNA motif in the 3' end of the genomes of astroviruses, avian infectious bronchitis virus and an equine rhinovirus. J. Gen. Virol. 79 (Pt 4), 715–718. https://doi.org/10.1099/0022-1317-79-4-715

Justa-Schuch, D., Silva-Garcia, M., Pilla, E., Engelke, M., Kilisch, M., Lenz, C., Möller, U., Nakamura, F., Urlaub, H., Geiss-Friedlander, R., 2016. DPP9 is a novel component of the N-end rule pathway targeting the tyrosine kinase Syk. eLife 5, e16370. https://doi.org/10.7554/eLife.16370

Kang, H., Feng, M., Schroeder, M.E., Giedroc, D.P., Leibowitz, J.L., 2006. Stem-loop 1 in the 5' UTR of the SARS coronavirus can substitute for its counterpart in mouse hepatitis virus. Adv. Exp. Med. Biol. 581, 105–108. https://doi.org/10.1007/978-0-387-33012-9_18

Karagöz, G.E., Acosta-Alvear, D., Walter, P., 2019. The Unfolded Protein Response: Detecting and Responding to Fluctuations in the Protein-Folding Capacity of the Endoplasmic Reticulum. Cold Spring Harb. Perspect. Biol. 11, a033886. https://doi.org/10.1101/cshperspect.a033886

Kelemen, O., Convertini, P., Zhang, Z., Wen, Y., Shen, M., Falaleeva, M., Stamm, S., 2013. Function of alternative splicing. Gene 514, 1–30. https://doi.org/10.1016/j.gene.2012.07.083

Kelly, J.A., Olson, A.N., Neupane, K., Munshi, S., San Emeterio, J., Pollack, L., Woodside, M.T., Dinman, J.D., 2020. Structural and functional conservation of the programmed −1 ribosomal frameshift signal of SARS coronavirus 2 (SARS-CoV-2). J. Biol. Chem. 295, 10741–10748. https://doi.org/10.1074/jbc.AC120.013449

Kemmerer, K., Fischer, S., Weigand, J.E., 2018. Auto- and cross-regulation of the hnRNPs D and DL. RNA 24, 324–331. https://doi.org/10.1261/rna.063420.117

Kemmerer, K., Weigand, J.E., 2014. Hypoxia reduces MAX expression in endothelial cells by unproductive splicing. FEBS Lett. 588, 4784–4790. https://doi.org/10.1016/j.febslet.2014.11.011

Kim, H.K., Pham, M.H.C., Ko, K.S., Rhee, B.D., Han, J., 2018. Alternative splicing isoforms in health and disease. Pflüg. Arch. - Eur. J. Physiol. 470, 995–1016. https://doi.org/10.1007/s00424-018-2136-x

Kim, Y.-C., Snoberger, A., Schupp, J., Smith, D.M., 2015. ATP binding to neighbouring subunits and intersubunit allosteric coupling underlie proteasomal ATPase function. Nat. Commun. 6, 8520. https://doi.org/10.1038/ncomms9520

Kopito, R.R., 2000. Aggresomes, inclusion bodies and protein aggregation. Trends Cell Biol. 10, 524–530. https://doi.org/10.1016/S0962-8924(00)01852-3

Koren, I., Timms, R.T., Kula, T., Xu, Q., Li, M.Z., Elledge, S.J., 2018. The Eukaryotic Proteome Is Shaped by E3 Ubiquitin Ligases Targeting C-Terminal Degrons. Cell 173, 1622-1635.e14. https://doi.org/10.1016/j.cell.2018.04.028

Kovacs, E., Tompa, P., Liliom, K., Kalmar, L., 2010. Dual coding in alternative reading frames correlates with intrinsic protein disorder. Proc. Natl. Acad. Sci. U. S. A. 107, 5429–5434. https://doi.org/10.1073/pnas.0907841107

Kumar, S., Maurya, V.K., Prasad, A.K., Bhatt, M.L.B., Saxena, S.K., 2020. Structural, glycosylation and antigenic variation between 2019 novel coronavirus (2019-nCoV) and SARS coronavirus (SARS-CoV). VirusDisease 31, 13–21. https://doi.org/10.1007/s13337-020-00571-5

Kurosaki, T., Popp, M.W., Maquat, L.E., 2019. Quality and quantity control of gene expression by nonsense-mediated mRNA decay. Nat. Rev. Mol. Cell Biol. 20, 406–420. https://doi.org/10.1038/s41580-019-0126-2

Kusmierczyk, A.R., Kunjappu, M.J., Kim, R.Y., Hochstrasser, M., 2011. A Conserved 20S Proteasome Assembly Factor Requires a C-terminal HbYX Motif for Proteasomal Precursor Binding. Nat. Struct. Mol. Biol. 18, 622–629. https://doi.org/10.1038/nsmb.2027

Lal, A., Mazan-Mamczarz, K., Kawai, T., Yang, X., Martindale, J.L., Gorospe, M., 2004. Concurrent versus individual binding of HuR and AUF1 to common labile target mRNAs. EMBO J. 23, 3092–3102. https://doi.org/10.1038/sj.emboj.7600305

Langklotz, S., Baumann, U., Narberhaus, F., 2012. Structure and function of the bacterial AAA protease FtsH. Biochim. Biophys. Acta BBA - Mol. Cell Res., AAA ATPases: structure and function 1823, 40–48. https://doi.org/10.1016/j.bbamcr.2011.08.015

Lapointe, C.P., Grosely, R., Johnson, A.G., Wang, J., Fernández, I.S., Puglisi, J.D., 2021. Dynamic competition between SARS-CoV-2 NSP1 and mRNA on the human ribosome inhibits translation initiation. Proc. Natl. Acad. Sci. U. S. A. 118, e2017715118. https://doi.org/10.1073/pnas.2017715118

Larsson, L.-G., Bahram, F., Burkhardt, H., Lüscher, B., 1997. Analysis of the DNA-binding activities of Myc/Max/Mad network complexes during induced differentiation of U-937 monoblasts and F9 teratocarcinoma cells. Oncogene 15, 737–748. https://doi.org/10.1038/sj.onc.1201390

Lee, J.W., Ko, J., Ju, C., Eltzschig, H.K., 2019. Hypoxia signaling in human diseases and therapeutic targets. Exp. Mol. Med. 51, 1–13. https://doi.org/10.1038/s12276-019-0235-1

Leon, J., Ferrandiz, N., Acosta, J.C., Delgado, M.D., 2009. Inhibition of cell differentiation: A critical mechanism for MYC-mediated carcinogenesis? Cell Cycle 8, 1148–1157. https://doi.org/10.4161/cc.8.8.8126

Leppek, K., Schott, J., Reitter, S., Poetz, F., Hammond, M.C., Stoecklin, G., 2013. Roquin promotes constitutive mRNA decay via a conserved class of stem-loop recognition motifs. Cell 153, 869–881. https://doi.org/10.1016/j.cell.2013.04.016

Lewis, B.P., Green, R.E., Brenner, S.E., 2003. Evidence for the widespread coupling of alternative splicing and nonsense-mediated mRNA decay in humans. Proc. Natl. Acad. Sci. U. S. A. 100, 189–192. https://doi.org/10.1073/pnas.0136770100

Li, L., Kang, H., Liu, P., Makkinje, N., Williamson, S.T., Leibowitz, J.L., Giedroc, D.P., 2008. Structural lability in stem-loop 1 drives a 5′ UTR-3′ UTR interaction in coronavirus replication. J. Mol. Biol. 377, 790–803. https://doi.org/10.1016/j.jmb.2008.01.068

Li, W., Li, Y., Guan, S., Fan, J., Cheng, C.-F., Bright, A.M., Chinn, C., Chen, M., Woodley, D.T., 2007. Extracellular heat shock protein-90alpha: linking hypoxia to skin cell motility and wound healing. EMBO J. 26, 1221–1233. https://doi.org/10.1038/sj.emboj.7601579

Li, Y., Garcia, G., Arumugaswami, V., Guo, F., 2021. Structure-based design of antisense oligonucleotides that inhibit SARS-CoV-2 replication. https://doi.org/10.1101/2021.08.23.457434

Li, Y.E., Xiao, M., Shi, B., Yang, Y.-C.T., Wang, D., Wang, F., Marcia, M., Lu, Z.J., 2017. Identification of high-confidence RNA regulatory elements by combinatorial classification of RNA–protein binding sites. Genome Biol. 18, 169. https://doi.org/10.1186/s13059-017-1298-8

Lin, H.-C., Yeh, C.-W., Chen, Y.-F., Lee, T.-T., Hsieh, P.-Y., Rusnac, D.V., Lin, S.-Y., Elledge, S.J., Zheng, N., Yen, H.-C.S., 2018. C-Terminal End-Directed Protein Elimination by CRL2 Ubiquitin Ligases. Mol. Cell 70, 602-613.e3. https://doi.org/10.1016/j.molcel.2018.04.006

Liu, P., Li, L., Millership, J.J., Kang, H., Leibowitz, J.L., Giedroc, D.P., 2007. A U-turn motif-containing stem-loop in the coronavirus 5' untranslated region plays a functional role in replication. RNA N. Y. N 13, 763–780. https://doi.org/10.1261/rna.261807

Livneh, I., Cohen-Kaplan, V., Cohen-Rosenzweig, C., Avni, N., Ciechanover, A., 2016. The life cycle of the 26S proteasome: from birth, through regulation and function, and onto its death. Cell Res. 26, 869–885. https://doi.org/10.1038/cr.2016.86

Loflin, P., Chen, C.-Y.A., Shyu, A.-B., 1999. Unraveling a cytoplasmic role for hnRNP D in the in vivo mRNA destabilization directed by the AU-rich element. Genes Dev. 13, 1884–1897.

Long, J.C., Caceres, J.F., 2009. The SR protein family of splicing factors: master regulators of gene expression. Biochem. J. 417, 15–27. https://doi.org/10.1042/BJ20081501

Lulla, V., Wandel, M.P., Bandyra, K.J., Ulferts, R., Wu, M., Dendooven, T., Yang, X., Doyle, N., Oerum, S., Beale, R., O'Rourke, S.M., Randow, F., Maier, H.J., Scott, W., Ding, Y., Firth, A.E., Bloznelyte, K., Luisi, B.F., 2021. Targeting the Conserved Stem Loop 2 Motif in the SARS-CoV-2 Genome. J. Virol. 95, e00663-21. https://doi.org/10.1128/JVI.00663-21

Madhugiri, R., Fricke, M., Marz, M., Ziebuhr, J., 2016. Coronavirus cis-Acting RNA Elements, in: Advances in Virus Research. Elsevier, pp. 127–163. https://doi.org/10.1016/bs.aivir.2016.08.007

Madhugiri, R., Karl, N., Petersen, D., Lamkiewicz, K., Fricke, M., Wend, U., Scheuer, R., Marz, M., Ziebuhr, J., 2018. Structural and functional conservation of cis-acting RNA elements in coronavirus 5'-terminal genome regions. Virology 517, 44–55. https://doi.org/10.1016/j.virol.2017.11.025

Makino, Y., Cao, R., Svensson, K., Bertilsson, G., Asman, M., Tanaka, H., Cao, Y., Berkenstam, A., Poellinger, L., 2001. Inhibitory PAS domain protein is a negative regulator of hypoxia-inducible gene expression. Nature 414, 550–554. https://doi.org/10.1038/35107085

Manfredonia, I., Incarnato, D., 2021. Structure and regulation of coronavirus genomes: state-of-the-art and novel insights from SARS-CoV-2 studies. Biochem. Soc. Trans. 49, 341–352. https://doi.org/10.1042/BST20200670

Manfredonia, I., Nithin, C., Ponce-Salvatierra, A., Ghosh, P., Wirecki, T.K., Marinus, T., Ogando, N.S., Snijder, E.J., van Hemert, M.J., Bujnicki, J.M., Incarnato, D., 2020. Genome-wide mapping of SARS-CoV-2 RNA structures identifies therapeutically-relevant elements. Nucleic Acids Res. 48, 12436–12452. https://doi.org/10.1093/nar/gkaa1053

Masters, P.S., 2019. Coronavirus genomic RNA packaging. Virology 537, 198–207. https://doi.org/10.1016/j.virol.2019.08.031

Mathsyaraja, H., Freie, B., Cheng, P.-F., Babaeva, E., Catchpole, J.T., Janssens, D., Henikoff, S., Eisenman, R.N., 2019. Max deletion destabilizes MYC protein and abrogates Eμ-Myc lymphomagenesis. Genes Dev. 33, 1252–1264. https://doi.org/10.1101/gad.325878.119

Matsye, P., Zheng, L., Si, Y., Kim, S., Luo, W., Crossman, D.K., Bratcher, P.E., King, P.H., 2017. HuR promotes the molecular signature and phenotype of activated microglia: Implications for amyotrophic lateral sclerosis and other neurodegenerative diseases. Glia 65, 945–963. https://doi.org/10.1002/glia.23137

Maynard, M.A., Evans, A.J., Shi, W., Kim, W.Y., Liu, F.-F., Ohh, M., 2007. Dominant-negative HIF-3 alpha 4 suppresses VHL-null renal cell carcinoma progression. Cell Cycle Georget. Tex 6, 2810–2816. https://doi.org/10.4161/cc.6.22.4947

McKinnon, C., Tabrizi, S.J., 2014. The Ubiquitin-Proteasome System in Neurodegeneration. Antioxid. Redox Signal. 21, 2302–2321. https://doi.org/10.1089/ars.2013.5802

McMahon, S.B., Van Buskirk, H.A., Dugan, K.A., Copeland, T.D., Cole, M.D., 1998. The Novel ATM-Related Protein TRRAP Is an Essential Cofactor for the c-Myc and E2F Oncoproteins. Cell 94, 363–374. https://doi.org/10.1016/S0092-8674(00)81479-8

McMahon, S.B., Wood, M.A., Cole, M.D., 2000. The Essential Cofactor TRRAP Recruits the Histone Acetyltransferase hGCN5 to c-Myc. Mol. Cell. Biol. 20, 556–562.

McManus, C.J., Graveley, B.R., 2011. RNA structure and the mechanisms of alternative splicing. Curr. Opin. Genet. Dev. 21, 373–379. https://doi.org/10.1016/j.gde.2011.04.001

Mehrtash, A.B., Hochstrasser, M., 2019. Ubiquitin-dependent Protein Degradation at the Endoplasmic Reticulum and Nuclear Envelope. Semin. Cell Dev. Biol. 93, 111–124. https://doi.org/10.1016/j.semcdb.2018.09.013

Meijer, T.W.H., Kaanders, J.H.A.M., Span, P.N., Bussink, J., 2012. Targeting Hypoxia, HIF-1, and Tumor Glucose Metabolism to Improve Radiotherapy Efficacy. Clin. Cancer Res. 18, 5585–5594. https://doi.org/10.1158/1078-0432.CCR-12-0858

Mino, T., Murakawa, Y., Fukao, A., Vandenbon, A., Wessels, H.-H., Ori, D., Uehata, T., Tartey, S., Akira, S., Suzuki, Y., Vinuesa, C.G., Ohler, U., Standley, D.M., Landthaler, M., Fujiwara, T., Takeuchi, O., 2015. Regnase-1 and Roquin Regulate a Common Element in Inflammatory mRNAs by Spatiotemporally Distinct Mechanisms. Cell 161, 1058–1073. https://doi.org/10.1016/j.cell.2015.04.029

Mino, T., Takeuchi, O., 2018. Post-transcriptional regulation of immune responses by RNA binding proteins. Proc. Jpn. Acad. Ser. B Phys. Biol. Sci. 94, 248–258. https://doi.org/10.2183/pjab.94.017

Müller-McNicoll, M., Rossbach, O., Hui, J., Medenbach, J., 2019. Auto-regulatory feedback by RNA-binding proteins. J. Mol. Cell Biol. 11, 930–939. https://doi.org/10.1093/jmcb/mjz043

Murakawa, Y., Hinz, M., Mothes, J., Schuetz, A., Uhl, M., Wyler, E., Yasuda, T., Mastrobuoni, G., Friedel, C.C., Dölken, L., Kempa, S., Schmidt-Supprian, M., Blüthgen, N., Backofen, R., Heinemann, U., Wolf, J., Scheidereit, C., Landthaler, M., 2015. RC3H1 post-transcriptionally regulates A20 mRNA and modulates the activity of the IKK/NF-κB pathway. Nat. Commun. 6, 7367. https://doi.org/10.1038/ncomms8367

Muz, B., de la Puente, P., Azab, F., Azab, A.K., 2015. The role of hypoxia in cancer progression, angiogenesis, metastasis, and resistance to therapy. Hypoxia 3, 83–92. https://doi.org/10.2147/HP.S93413

Nair, S.K., Burley, S.K., 2003. X-Ray Structures of Myc-Max and Mad-Max Recognizing DNA: Molecular Bases of Regulation by Proto-Oncogenic Transcription Factors. Cell 112, 193–205. https://doi.org/10.1016/S0092-8674(02)01284-9

Pagliarini, V., Naro, C., Sette, C., 2015. Splicing Regulation: A Molecular Device to Enhance Cancer Cell Adaptation. BioMed Res. Int. 2015, e543067. https://doi.org/10.1155/2015/543067

Peter, S.A., Isaac, J.S., Narberhaus, F., Weigand, J.E., 2021. A novel, universally active C-terminal protein degradation signal generated by alternative splicing. J. Mol. Biol. 166890. https://doi.org/10.1016/j.jmb.2021.166890

Piasecka, A., Czapinska, H., Vielberg, M.-T., Szczepanowski, R.H., Kiefersauer, R., Reed, S., Groll, M., Bochtler, M., 2018. The Y. bercovieri Anbu crystal structure sheds light on the evolution of

highly (pseudo)symmetric multimers. J. Mol. Biol. 430, 611–627. https://doi.org/10.1016/j.jmb.2017.11.016

Pickering, A.M., Davies, K.J.A., 2012. Differential roles of proteasome and immunoproteasome regulators Pa28αβ, Pa28γ and Pa200 in the degradation of oxidized proteins. Arch. Biochem. Biophys. 523, 181–190. https://doi.org/10.1016/j.abb.2012.04.018

Plant, E.P., Rakauskaitė, R., Taylor, D.R., Dinman, J.D., 2010. Achieving a Golden Mean: Mechanisms by Which Coronaviruses Ensure Synthesis of the Correct Stoichiometric Ratios of Viral Proteins. J. Virol. 84, 4330–4340. https://doi.org/10.1128/JVI.02480-09

Pohl, E.E., Rupprecht, A., Macher, G., Hilse, K.E., 2019. Important Trends in UCP3 Investigation. Front. Physiol. 10, 470. https://doi.org/10.3389/fphys.2019.00470

Pohl, M., Bortfeldt, R.H., Grützmann, K., Schuster, S., 2013. Alternative splicing of mutually exclusive exons—A review. Biosystems 114, 31–38. https://doi.org/10.1016/j.biosystems.2013.07.003

Potente, M., Gerhardt, H., Carmeliet, P., 2011. Basic and therapeutic aspects of angiogenesis. Cell 146, 873–887. https://doi.org/10.1016/j.cell.2011.08.039

Preussner, M., Gao, Q., Morrison, E., Herdt, O., Finkernagel, F., Schumann, M., Krause, E., Freund, C., Chen, W., Heyd, F., 2020. Splicing-accessible coding 3′UTRs control protein stability and interaction networks. Genome Biol. 21, 186. https://doi.org/10.1186/s13059-020-02102-3

Quéva, C., Hurlin, P.J., Foley, K.P., Eisenman, R.N., 1998. Sequential expression of the MAD family of transcriptional repressors during differentiation and development. Oncogene 16, 967–977. https://doi.org/10.1038/sj.onc.1201611

Rabbitts, P. h., Watson, J. v., Lamond, A., Forster, A., Stinson, M. a., Evan, G., Fischer, W., Atherton, E., Sheppard, R., Rabbitts, T. h., 1985. Metabolism of c-myc gene products: c-myc mRNA and protein expression in the cell cycle. EMBO J. 4, 2009–2015. https://doi.org/10.1002/j.1460-2075.1985.tb03885.x

Rambout, X., Dequiedt, F., Maquat, L.E., 2018. Beyond Transcription: Roles of Transcription Factors in Pre-mRNA Splicing. Chem. Rev. 118, 4339–4364. https://doi.org/10.1021/acs.chemrev.7b00470

Rangan, R., Watkins, A.M., Chacon, J., Kretsch, R., Kladwang, W., Zheludev, I.N., Townley, J., Rynge, M., Thain, G., Das, R., 2021. De novo 3D models of SARS-CoV-2 RNA elements from consensus experimental secondary structures. Nucleic Acids Res. 49, 3092–3108. https://doi.org/10.1093/nar/gkab119

Rangan, R., Zheludev, I.N., Hagey, R.J., Pham, E.A., Wayment-Steele, H.K., Glenn, J.S., Das, R., 2020. RNA genome conservation and secondary structure in SARS-CoV-2 and SARS-related viruses: a first look. RNA 26, 937–959. https://doi.org/10.1261/rna.076141.120

Rehage, N., Davydova, E., Conrad, C., Behrens, G., Maiser, A., Stehklein, J.E., Brenner, S., Klein, J., Jeridi, A., Hoffmann, A., Lee, E., Dianzani, U., Willemsen, R., Feederle, R., Reiche, K., Hackermüller, J., Leonhardt, H., Sharma, S., Niessing, D., Heissmeyer, V., 2018. Binding of NUFIP2 to Roquin promotes recognition and regulation of ICOS mRNA. Nat. Commun. 9, 299. https://doi.org/10.1038/s41467-017-02582-1

Rezagholizadeh, A., Khiali, S., Sarbakhsh, P., Entezari-Maleki, T., 2021. Remdesivir for treatment of COVID-19; an updated systematic review and meta-analysis. Eur. J. Pharmacol. 897, 173926. https://doi.org/10.1016/j.ejphar.2021.173926

Robertson, M.P., Igel, H., Baertsch, R., Haussler, D., Ares, M., Scott, W.G., 2005. The structure of a rigorously conserved RNA element within the SARS virus genome. PLoS Biol. 3, e5. https://doi.org/10.1371/journal.pbio.0030005

Romano, M., Ruggiero, A., Squeglia, F., Maga, G., Berisio, R., 2020. A Structural View of SARS-CoV-2 RNA Replication Machinery: RNA Synthesis, Proofreading and Final Capping. Cells 9, 1267. https://doi.org/10.3390/cells9051267

Romero, O.A., Torres-Diz, M., Pros, E., Savola, S., Gomez, A., Moran, S., Saez, C., Iwakawa, R., Villanueva, A., Montuenga, L.M., Kohno, T., Yokota, J., Sanchez-Cespedes, M., 2014. MAX Inactivation in Small Cell Lung Cancer Disrupts MYC–SWI/SNF Programs and Is Synthetic Lethal with BRG1. Cancer Discov. 4, 292–303. https://doi.org/10.1158/2159-8290.CD-13-0799

Rosenke, K., Leventhal, S., Moulton, H.M., Hatlevig, S., Hawman, D., Feldmann, H., Stein, D.A., 2020. Inhibition of SARS-CoV-2 in Vero cell cultures by peptide-conjugated morpholino oligomers. J. Antimicrob. Chemother. dkaa460. https://doi.org/10.1093/jac/dkaa460

Sammak, S., Hamdani, N., Gorrec, F., Allen, M.D., Freund, S.M.V., Bycroft, M., Zinzalla, G., 2019. Crystal Structures and Nuclear Magnetic Resonance Studies of the Apo Form of the c-MYC:MAX bHLHZip Complex Reveal a Helical Basic Region in the Absence of DNA. Biochemistry 58, 3144–3154. https://doi.org/10.1021/acs.biochem.9b00296

Sauer, R.T., Baker, T.A., 2011. AAA+ Proteases: ATP-Fueled Machines of Protein Destruction. Annu. Rev. Biochem. 80, 587–612. https://doi.org/10.1146/annurev-biochem-060408-172623

Schaefer, J.S., Klein, J.R., 2016. Roquin – a multifunctional regulator of immune homeostasis. Genes Immun. 17, 79–84. https://doi.org/10.1038/gene.2015.58

Schito, L., Semenza, G.L., 2016. Hypoxia-Inducible Factors: Master Regulators of Cancer Progression. Trends Cancer 2, 758–770. https://doi.org/10.1016/j.trecan.2016.10.016

Schlundt, A., Heinz, G.A., Janowski, R., Geerlof, A., Stehle, R., Heissmeyer, V., Niessing, D., Sattler, M., 2014. Structural basis for RNA recognition in roquin-mediated post-transcriptional gene regulation. Nat. Struct. Mol. Biol. 21, 671–678. https://doi.org/10.1038/nsmb.2855

Schlundt, A., Niessing, D., Heissmeyer, V., Sattler, M., 2016. RNA recognition by Roquin in posttranscriptional gene regulation. Wiley Interdiscip. Rev. RNA 7, 455–469. https://doi.org/10.1002/wrna.1333

Schmidt, M., Finley, D., 2014. Regulation of proteasome activity in health and disease. Biochim. Biophys. Acta BBA - Mol. Cell Res., Ubiquitin-Proteasome System 1843, 13–25. https://doi.org/10.1016/j.bbamcr.2013.08.012

Schnieders, R., Peter, S.A., Banijamali, E., Riad, M., Altincekic, N., Bains, J.K., Ceylan, B., Fürtig, B., Grün, J.T., Hengesbach, M., Hohmann, K.F., Hymon, D., Knezic, B., Oxenfarth, A., Petzold, K., Qureshi, N.S., Richter, C., Schlagnitweit, J., Schlundt, A., Schwalbe, H., Stirnal, E., Sudakov, A., Vögele, J., Wacker, A., Weigand, J.E., Wirmer-Bartoschek, J., Wöhnert, J., 2021. 1H, 13C and 15N chemical shift assignment of the stem-loop 5a from the 5′-UTR of SARS-CoV-2. Biomol. Nmr Assign. 15, 203–211. https://doi.org/10.1007/s12104-021-10007-w

Scotti, M.M., Swanson, M.S., 2016. RNA mis-splicing in disease. Nat. Rev. Genet. 17, 19–32. https://doi.org/10.1038/nrg.2015.3

Semenza, G.L., 2017. HIF-1 and human disease: one highly involved factor. Genes Dev. 14:1983-1991, 10.

Sgromo, A., Raisch, T., Bawankar, P., Bhandari, D., Chen, Y., Kuzuoğlu-Öztürk, D., Weichenrieder, O., Izaurralde, E., 2017. A CAF40-binding motif facilitates recruitment of the CCR4-NOT complex to mRNAs targeted by Drosophila Roquin. Nat. Commun. 8, 14307. https://doi.org/10.1038/ncomms14307

Shi, M., Wang, L., Fontana, P., Vora, S., Zhang, Y., Fu, T.-M., Lieberman, J., Wu, H., 2020. SARS-CoV-2 Nsp1 suppresses host but not viral translation through a bipartite mechanism. bioRxiv 2020.09.18.302901. https://doi.org/10.1101/2020.09.18.302901

Shyu, A.-B., Wilkinson, M.F., van Hoof, A., 2008. Messenger RNA regulation: to translate or to degrade. EMBO J. 27, 471–481. https://doi.org/10.1038/sj.emboj.7601977

Sicoli, G., Vezin, H., Ledolter, K., Kress, T., Kurzbach, D., 2019. Conformational tuning of a DNA-bound transcription factor. Nucleic Acids Res. 47, 5429–5435. https://doi.org/10.1093/nar/gkz291

Simonson, T.S., Yang, Y., Huff, C.D., Yun, H., Qin, G., Witherspoon, D.J., Bai, Z., Lorenzo, F.R., Xing, J., Jorde, L.B., Prchal, J.T., Ge, R., 2010. Genetic Evidence for High-Altitude Adaptation in Tibet. Science 329, 72–75. https://doi.org/10.1126/science.1189406

Slobodin, B., Sehrawat, U., Lev, A., Ogran, A., Fraticelli, D., Hayat, D., Zuckerman, B., Ulitsky, I., Ben-Shmuel, A., Bar-David, E., Levy, H., Dikstein, R., 2021. Cap-independent translation and a precisely localized RNA sequence enable SARS-CoV-2 to control host translation and escape anti-viral response. https://doi.org/10.1101/2021.08.18.456855

Song, Y., Song, J., Wei, X., Huang, M., Sun, M., Zhu, L., Lin, B., Shen, H., Zhu, Z., Yang, C., 2020. Discovery of Aptamers Targeting the Receptor-Binding Domain of the SARS-CoV-2 Spike Glycoprotein. Anal. Chem. acs.analchem.0c01394. https://doi.org/10.1021/acs.analchem.0c01394

Sreeramulu, S., Richter, C., Berg, H., Wirtz Martin, M.A., Ceylan, B., Matzel, T., Adam, J., Altincekic, N., Azzaoui, K., Bains, J.K., Blommers, M.J.J., Ferner, J., Fürtig, B., Göbel, M., Grün, J.T., Hengesbach, M., Hohmann, K.F., Hymon, D., Knezic, B., Martins, J., Mertinkus, K.R., Niesteruk, A., Peter, S.A., Pyper, D.J., Qureshi, N.S., Scheffer, U., Schlundt, A., Schnieders, R., Stirnal, E., Sudakov, A., Tröster, A., Vögele, J., Wacker, A., Weigand, J.E., Wirmer-Bartoschek, J., Wöhnert, J., Schwalbe, H., 2021. Exploring the druggability of conserved RNA regulatory elements in the SARS-CoV-2 genome. Angew. Chem. Int. Ed Engl. https://doi.org/10.1002/anie.202103693

Srikantan, S., Tominaga, K., Gorospe, M., 2012. Functional interplay between RNA-binding protein HuR and microRNAs. Curr. Protein Pept. Sci. 13, 372–379. https://doi.org/10.2174/138920312801619394

Sterne-Weiler, T., Sanford, J.R., 2014. Exon identity crisis: disease-causing mutations that disrupt the splicing code. Genome Biol. 15, 201. https://doi.org/10.1186/gb4150

Strub, C., Alies, C., Lougarre, A., Ladurantie, C., Czaplicki, J., Fournier, D., 2004. Mutation of exposed hydrophobic amino acids to arginine to increase protein stability. BMC Biochem. 5, 9. https://doi.org/10.1186/1471-2091-5-9

Sun, M., Liu, S., Wei, X., Wan, S., Huang, M., Song, T., Lu, Y., Weng, X., Lin, Z., Chen, H., Song, Y., Yang, C., 2021. Aptamer Blocking Strategy Inhibits SARS-CoV-2 Virus Infection. Angew. Chem. Int. Ed Engl. 10.1002/anie.202100225. https://doi.org/10.1002/anie.202100225

Szemiel, A.M., Merits, A., Orton, R.J., MacLean, O.A., Pinto, R.M., Wickenhagen, A., Lieber, G., Turnbull, M.L., Wang, S., Furnon, W., Suarez, N.M., Mair, D., da Silva Filipe, A., Willett, B.J., Wilson, S.J., Patel, A.H., Thomson, E.C., Palmarini, M., Kohl, A., Stewart, M.E., 2021. In vitro selection of Remdesivir resistance suggests evolutionary predictability of SARS-CoV-2. PLoS Pathog. 17, e1009929. https://doi.org/10.1371/journal.ppat.1009929

Takahashi, K., Yamanaka, S., 2006. Induction of Pluripotent Stem Cells from Mouse Embryonic and Adult Fibroblast Cultures by Defined Factors. Cell 126, 663–676. https://doi.org/10.1016/j.cell.2006.07.024

Tan, D., Zhou, M., Kiledjian, M., Tong, L., 2014. The ROQ domain of Roquin recognizes mRNA constitutive-decay element and double-stranded RNA. Nat. Struct. Mol. Biol. 21, 679–685. https://doi.org/10.1038/nsmb.2857

Tanaka, T., Wiesener, M., Bernhardt, W., Eckardt, K.-U., Warnecke, C., 2009. The human HIF (hypoxia-inducible factor)-3alpha gene is a HIF-1 target gene and may modulate hypoxic gene induction. Biochem. J. 424, 143–151. https://doi.org/10.1042/BJ20090120

Tasaki, T., Kwon, Y.T., 2007. The mammalian N-end rule pathway: new insights into its components and physiological roles. Trends Biochem. Sci. 32, 520–528. https://doi.org/10.1016/j.tibs.2007.08.010

Tasaki, T., Mulder, L.C.F., Iwamatsu, A., Lee, M.J., Davydov, I.V., Varshavsky, A., Muesing, M., Kwon, Y.T., 2005. A Family of Mammalian E3 Ubiquitin Ligases That Contain the UBR Box Motif and Recognize N-Degrons. Mol. Cell. Biol. 25, 7120–7136. https://doi.org/10.1128/MCB.25.16.7120-7136.2005

Tazi, J., Bakkour, N., Stamm, S., 2009. Alternative splicing and disease. Biochim. Biophys. Acta BBA - Mol. Basis Dis. 1792, 14–26. https://doi.org/10.1016/j.bbadis.2008.09.017

Tengs, T., Jonassen, C.M., 2016. Distribution and Evolutionary History of the Mobile Genetic Element s2m in Coronaviruses. Dis. Basel Switz. 4, E27. https://doi.org/10.3390/diseases4030027

Tengs, T., Kristoffersen, A.B., Bachvaroff, T.R., Jonassen, C.M., 2013. A mobile genetic element with unknown function found in distantly related viruses. Virol. J. 10, 132. https://doi.org/10.1186/1743-422X-10-132

Tian, L., Qiang, T., Liang, C., Ren, X., Jia, M., Zhang, J., Li, J., Wan, M., YuWen, X., Li, H., Cao, W., Liu, H., 2021. RNA-dependent RNA polymerase (RdRp) inhibitors: The current landscape and repurposing for the COVID-19 pandemic. Eur. J. Med. Chem. 213, 113201. https://doi.org/10.1016/j.ejmech.2021.113201

Tidu, A., Janvier, A., Schaeffer, L., Sosnowski, P., Kuhn, L., Hammann, P., Westhof, E., Eriani, G., Martin, F., 2021. The viral protein NSP1 acts as a ribosome gatekeeper for shutting down host translation and fostering SARS-CoV-2 translation. RNA 27, 253–264. https://doi.org/10.1261/rna.078121.120

Timms, R.T., Koren, I., 2020. Tying up loose ends: the N-degron and C-degron pathways of protein degradation. Biochem. Soc. Trans. 48, 1557–1567. https://doi.org/10.1042/BST20191094

Ting, Y., Medina, D.J., Strair, R.K., Schaar, D.G., 2010. Differentiation-associated miR-22 represses Max expression and inhibits cell cycle progression. Biochem. Biophys. Res. Commun. 394, 606–611. https://doi.org/10.1016/j.bbrc.2010.03.030

Tomko, R.J., Hochstrasser, M., 2013. Molecular architecture and assembly of the eukaryotic proteasome. Annu. Rev. Biochem. 82, 415–445. https://doi.org/10.1146/annurev-biochem-060410-150257

Tomoyasu, T., Mogk, A., Langen, H., Goloubinoff, P., Bukau, B., 2001. Genetic dissection of the roles of chaperones and proteases in protein folding and degradation in the Escherichia coli cytosol. Mol. Microbiol. 40, 397–413. https://doi.org/10.1046/j.1365-2958.2001.02383.x

Trobaugh, D.W., Gardner, C.L., Sun, C., Haddow, A.D., Wang, E., Chapnik, E., Mildner, A., Weaver, S.C., Ryman, K.D., Klimstra, W.B., 2014. RNA viruses can hijack vertebrate microRNAs to suppress innate immunity. Nature 506, 245–248. https://doi.org/10.1038/nature12869

Truscott, K.N., Bezawork-Geleta, A., Dougan, D.A., 2011. Unfolded protein responses in bacteria and mitochondria: A central role for the ClpXP machine. IUBMB Life 63, 955–963. https://doi.org/10.1002/iub.526

Ule, J., Blencowe, B.J., 2019. Alternative Splicing Regulatory Networks: Functions, Mechanisms, and Evolution. Mol. Cell 76, 329–345. https://doi.org/10.1016/j.molcel.2019.09.017

van der Lee, R., Lang, B., Kruse, K., Gsponer, J., Sánchez de Groot, N., Huynen, M.A., Matouschek, A., Fuxreiter, M., Babu, M.M., 2014. Intrinsically Disordered Segments Affect Protein Half-Life in the Cell and during Evolution. Cell Rep. 8, 1832–1844. https://doi.org/10.1016/j.celrep.2014.07.055

Varshavsky, A., 2019. N-degron and C-degron pathways of protein degradation. Proc. Natl. Acad. Sci. 116, 358–366. https://doi.org/10.1073/pnas.1816596116

Varshavsky, A., 2011. The N-end rule pathway and regulation by proteolysis. Protein Sci. Publ. Protein Soc. 20, 1298–1345. https://doi.org/10.1002/pro.666

Vembar, S.S., Brodsky, J.L., 2008. One step at a time: endoplasmic reticulum-associated degradation. Nat. Rev. Mol. Cell Biol. 9, 944–957. https://doi.org/10.1038/nrm2546

Vielberg, M.-T., Bauer, V.C., Groll, M., 2018. On the Trails of the Proteasome Fold: Structural and Functional Analysis of the Ancestral β-Subunit Protein Anbu. J. Mol. Biol. 430, 628–640. https://doi.org/10.1016/j.jmb.2018.01.004

Vinuesa, C.G., Cook, M.C., Angelucci, C., Athanasopoulos, V., Rui, L., Hill, K.M., Yu, D., Domaschenz, H., Whittle, B., Lambe, T., Roberts, I.S., Copley, R.R., Bell, J.I., Cornall, R.J., Goodnow, C.C., 2005. A RING-type ubiquitin ligase family member required to repress follicular helper T cells and autoimmunity. Nature 435, 452–458. https://doi.org/10.1038/nature03555

Vogel, K.U., Edelmann, S.L., Jeltsch, K.M., Bertossi, A., Heger, K., Heinz, G.A., Zöller, J., Warth, S.C., Hoefig, K.P., Lohs, C., Neff, F., Kremmer, E., Schick, J., Repsilber, D., Geerlof, A., Blum, H., Wurst, W., Heikenwälder, M., Schmidt-Supprian, M., Heissmeyer, V., 2013. Roquin Paralogs 1 and 2 Redundantly Repress the Icos and Ox40 Costimulator mRNAs and Control Follicular Helper T Cell Differentiation. Immunity 38, 655–668. https://doi.org/10.1016/j.immuni.2012.12.004

Vögele, J., Ferner, J.-P., Altincekic, N., Bains, J.K., Ceylan, B., Fürtig, B., Grün, J.T., Hengesbach, M., Hohmann, K.F., Hymon, D., Knezic, B., Löhr, F., Peter, S.A., Pyper, D., Qureshi, N.S., Richter, C., Schlundt, A., Schwalbe, H., Stirnal, E., Sudakov, A., Wacker, A., Weigand, J.E., Wirmer-Bartoschek, J., Wöhnert, J., Duchardt-Ferner, E., 2021. 1H, 13C, 15N and 31P chemical shift assignment for

stem-loop 4 from the 5′-UTR of SARS-CoV-2. Biomol. Nmr Assign. 1–6. https://doi.org/10.1007/s12104-021-10026-7

Vora, S.M., Fontana, P., Leger, V., Zhang, Y., Fu, T.-M., Lieberman, J., Gehrke, L., Shi, M., Wang, L., Wu, H., 2021. Targeting Stem-loop 1 of the SARS-CoV-2 5'UTR to suppress viral translation and Nsp1 evasion. https://doi.org/10.1101/2021.09.09.459641

Wacker, A., Weigand, J.E., Akabayov, S.R., Altincekic, N., Bains, J.K., Banijamali, E., Binas, O., Castillo-Martinez, J., Cetiner, E., Ceylan, B., Chiu, L.-Y., Davila-Calderon, J., Dhamotharan, K., Duchardt-Ferner, E., Ferner, J., Frydman, L., Fürtig, B., Gallego, J., Grün, J.T., Hacker, C., Haddad, C., Hähnke, M., Hengesbach, M., Hiller, F., Hohmann, K.F., Hymon, D., de Jesus, V., Jonker, H., Keller, H., Knezic, B., Landgraf, T., Löhr, F., Luo, L., Mertinkus, K.R., Muhs, C., Novakovic, M., Oxenfarth, A., Palomino-Schätzlein, M., Petzold, K., Peter, S.A., Pyper, D.J., Qureshi, N.S., Riad, M., Richter, C., Saxena, K., Schamber, T., Scherf, T., Schlagnitweit, J., Schlundt, A., Schnieders, R., Schwalbe, H., Simba-Lahuasi, A., Sreeramulu, S., Stirnal, E., Sudakov, A., Tants, J.-N., Tolbert, B.S., Vögele, J., Weiß, L., Wirmer-Bartoschek, J., Wirtz Martin, M.A., Wöhnert, J., Zetzsche, H., 2020. Secondary structure determination of conserved SARS-CoV-2 RNA elements by NMR spectroscopy. Nucleic Acids Res. 48, 12415–12435. https://doi.org/10.1093/nar/gkaa1013

Wahl, M.C., Will, C.L., Lührmann, R., 2009. The spliceosome: design principles of a dynamic RNP machine. Cell 136, 701–718. https://doi.org/10.1016/j.cell.2009.02.009

Wang, E.T., Sandberg, R., Luo, S., Khrebtukova, I., Zhang, L., Mayr, C., Kingsmore, S.F., Schroth, G.P., Burge, C.B., 2008. Alternative isoform regulation in human tissue transcriptomes. Nature 456, 470–476. https://doi.org/10.1038/nature07509

Wang, L., Wang, Y., Ye, D., Liu, Q., 2020. Review of the 2019 novel coronavirus (SARS-CoV-2) based on current evidence. Int. J. Antimicrob. Agents 55, 105948. https://doi.org/10.1016/j.ijantimicag.2020.105948

Weigand, J.E., Boeckel, J.-N., Gellert, P., Dimmeler, S., 2012. Hypoxia-Induced Alternative Splicing in Endothelial Cells. PLOS ONE 7, e42697. https://doi.org/10.1371/journal.pone.0042697

Wetzel, R., 1994. Mutations and off-pathway aggregation of proteins. Trends Biotechnol. 12, 193–198. https://doi.org/10.1016/0167-7799(94)90082-5

Will, C.L., Lührmann, R., 2011. Spliceosome Structure and Function. Cold Spring Harb. Perspect. Biol. 3. https://doi.org/10.1101/cshperspect.a003707

Williamson, B.N., Feldmann, F., Schwarz, B., Meade-White, K., Porter, D.P., Schulz, J., van Doremalen, N., Leighton, I., Yinda, C.K., Pérez-Pérez, L., Okumura, A., Lovaglio, J., Hanley, P.W., Saturday, G., Bosio, C.M., Anzick, S., Barbian, K., Cihlar, T., Martens, C., Scott, D.P., Munster, V.J., de Wit, E., 2020. Clinical benefit of remdesivir in rhesus macaques infected with SARS-CoV-2. Nature 585, 273–276. https://doi.org/10.1038/s41586-020-2423-5

Wilusz, C.J., Wormington, M., Peltz, S.W., 2001. The cap-to-tail guide to mRNA turnover. Nat. Rev. Mol. Cell Biol. 2, 237–246. https://doi.org/10.1038/35067025

Yamashita, T., Higashi, M., Momose, S., Adachi, A., Watanabe, T., Tanaka, Y., Tokuhira, M., Kizaki, M., Tamaru, J., 2020. Decreased MYC-associated factor X (MAX) expression is a new potential biomarker for adverse prognosis in anaplastic large cell lymphoma. Sci. Rep. 10. https://doi.org/10.1038/s41598-020-67500-w

Yang, D., Liu, P., Giedroc, D.P., Leibowitz, J., 2011. Mouse hepatitis virus stem-loop 4 functions as a spacer element required to drive subgenomic RNA synthesis. J. Virol. 85, 9199–9209. https://doi.org/10.1128/JVI.05092-11

Yang, G., Li, Z., Mohammed, I., Zhao, L., Wei, W., Xiao, H., Guo, W., Zhao, Y., Qu, F., Huang, Y., 2021. Identification of SARS-CoV-2-against aptamer with high neutralization activity by blocking the RBD domain of spike protein 1. Signal Transduct. Target. Ther. 6, 227. https://doi.org/10.1038/s41392-021-00649-6

Yedidi, R.S., Wendler, P., Enenkel, C., 2017. AAA-ATPases in Protein Degradation. Front. Mol. Biosci. 4, 42. https://doi.org/10.3389/fmolb.2017.00042

Yu, D., Tan, A.H.-M., Hu, X., Athanasopoulos, V., Simpson, N., Silva, D.G., Hutloff, A., Giles, K.M., Leedman, P.J., Lam, K.P., Goodnow, C.C., Vinuesa, C.G., 2007. Roquin represses autoimmunity by limiting inducible T-cell co-stimulator messenger RNA. Nature 450, 299–303. https://doi.org/10.1038/nature06253

Zervos, A.S., Gyuris, J., Brent, R., 1993. Mxi1, a protein that specifically interacts with Max to bind Myc-Max recognition sites. Cell 72, 223–232. https://doi.org/10.1016/0092-8674(93)90662-A

Zhao, J., Zhang, G., Zhang, Y., Yi, D., Li, Q., Ma, L., Guo, S., Li, X., Guo, F., Lin, R., Luu, G., Liu, Z., Wang, Y., Cen, S., 2021. 2-((1H-indol-3-yl)thio)-N-phenyl-acetamides: SARS-CoV-2 RNA-dependent RNA polymerase inhibitors. Antiviral Res. 196, 105209. https://doi.org/10.1016/j.antiviral.2021.105209

Zheng, Q., Huang, T., Zhang, L., Zhou, Y., Luo, H., Xu, H., Wang, X., 2016. Dysregulation of Ubiquitin-Proteasome System in Neurodegenerative Diseases. Front. Aging Neurosci. 8. https://doi.org/10.3389/fnagi.2016.00303

Zhou, X., Guo, X., Chen, M., Xie, C., Jiang, J., 2018. HIF-3α Promotes Metastatic Phenotypes in Pancreatic Cancer by Transcriptional Regulation of the RhoC-ROCK1 Signaling Pathway. Mol. Cancer Res. MCR 16, 124–134. https://doi.org/10.1158/1541-7786.MCR-17-0256

Ziv, O., Price, J., Shalamova, L., Kamenova, T., Goodfellow, I., Weber, F., Miska, E.A., 2020. The Short- and Long-Range RNA-RNA Interactome of SARS-CoV-2. Mol. Cell 80, 1067-1077.e5. https://doi.org/10.1016/j.molcel.2020.11.004

8. Abbreviations

RNA	ribonucleic acid
DNA	deoxyribonucleic acid
RBPs	RNA-binding proteins
AS	alternative splicing
S. cerevisiae	*Saccharomyces cerevisiae*
E. coli	*Escherichia coli*
SL	stem-loop
UTR	untranslated region
mRNA	messenger RNA
CDE	constitutive decay element
ARE	AU-rich element
ORF	open reading frame
PTM	posttranslational modification
snRNPs	small nuclear ribonucleoprotein particles
SS	splice site
nt	nucleotide
ESE	exonic splicing enhancer
ISE	intronic splicing enhancer
ISS	intronic splicing silencer
ESS	exonic splicing silencer
hnRNP	heterogenous nuclear ribonucleoprotein
ROS	reactive oxygen species
MXE	mutually exclusive exon
CE	cassette exon
A5SS	alternative 5'-splice site
A3SS	alternative 3'-splice site
IR	intron retention
SRE	splicing regulatory element
RRM	RNA recognition motif
RS domain	Arginine-Serine domain
NMD	nonsense-mediated decay
PTC	premature termination codon
HIF	hypoxia inducible factor
PHD	prolyl hydroxylase
VHL	Von Hippel-Lindau
ARNT	aryl hydrocarbon receptor nuclear translator
HRE	hypoxia responsive element
VEGF	vascular endothelial growth factor
MAX	Myc-associated factor X
bHLHLZ	basic helix-loop-helix-leucine-zipper
TAD	transcriptional activation domain
ALCL	anaplastic large cell lymphoma
PTCL-NOS	peripheral T-cell lymphoma

aa	amino acids
ATP	adenine tri-phosphate
RP	regulatory particle
CP	core particle
Rpn	regulatory non-ATPase subunit
Rpt	regulatory ATPase subunit
RING	really interesting new gene
PSR	proline-serine rich sequence
SARS-CoV-2	severe acute respiratory syndrome -coronavirus
CoV	coronavirus
PP1a	polyprotein 1a
Nsp	non-structural protein
sgRNA	subgenomic RNA
HVR	hypervariable region
MHV	mouse hepatitis virus
uORF	upstream ORF
att hp	attenuator hairpin
OMP	outer membrane protein

9. Acknowledgements

An dieser Stelle möchte ich mich bei all den Menschen bedanken, die mir geholfen haben diese Thesis einzureichen:

Dr. Julia Weigand:
Vielen Dank für all die Hilfe, sei es nun Korrektur oder in experimentellen Dingen. Danke für die Gespräche, ob privat oder wissenschaftlich, die super Betreuung und einfach nur dafür, dass ich immer zu Dir kommen konnte. Die Arbeit mit Dir hat mir immer viel Spaß gemacht.

Prof. Dr. Beatrix Süß:
Danke, dass ich meine Arbeit in Deiner Gruppe beginnen konnte. Die Ausflüge oder gemeinschaftlichen Aktionen waren immer toll und bleiben mir immer in guter Erinnerung. Danke, dass ich auch stets zu Dir kommen konnte.

Prof. Dr. Alexander Löwer:
Danke, dass Sie mein Prüfer waren und für die Ratschläge gerade am Anfang meiner Promotion.

Prof. Dr. Dieter Steinhilber:
Danke, dass Sie mein externer Prüfer waren.

Weigand-Lab:
Johannes: Danke, dass Du mich eingearbeitet hast und mir gezeigt hast, wie der Hase läuft.
Sandra: Danke für die Hilfe und gemeinsamen, lustigen Arbeitsstunden. Und die Gespräche über die Ticks unserer Katzen.
Britta: Danke für die Hilfe und Tricks

Chiara: Danke, dass Du mir die Vorzüge des Kaffees gezeigt hast und die lustigen Albereien
Lasse: Danke, dass Du die gemeinsamen Pausen mit Witz und Sprüchen gefüllt hast
Julian: Danke, dass Du mich unterstützt hast bei den Screens. Ich habe gerne mit Dir gearbeitet
Danke an alle ehemaligen Studenten von mir, vor allem an Bea, JD und Paul. Ihr wart echt super.
Danke an alle jetzigen Studenten des Weigand-Labs. Es war immer lustig mit Euch und ich konnte viel rumalbern mit Euch.

AG Saul:
Anett, Dorie, Eva und Kai: Danke, dass die Mittagspausen so witzig mit Euch waren und Ihr immer ein offenes Ohr hattet.

AG Süß:
Janis, Janice, Lisa, Leon, Robin: Danke, dass man mit Euch immer reden konnte.
Marc und Michi: Danke, dass Ihr die administrativen Aufgaben übernommen habt und dass Ihr die technischen Probleme immer beheben konntet.

Dunja
Vielen Dank, dass Du immer die Organisation von Verwaltungsangelegenheiten übernommen hast und immer so super weiter helfen konntest.

Meiner Familie:
Danke, dass Ihr mich immer unterstützt habt. Ohne Euch wäre ich vielleicht nicht so weit gekommen.

Meinen Freunden:
Danke, dass Ihr meine Freizeit so schön mit Leben gefüllt habt.

10. Contributions

This thesis is based on the following publications (in chronological order):

1. Binas O, Tants J-N, **Peter SA**, Janowski R, Davydova E, Braun J, Niessing D, Schwalbe H, Weigand JE and Schlundt A (2020). Structural basis for the recognition of transiently structured AU-rich elements by Roquin. Nucleic Acids Res 48, 7385-7403.

2. Wacker A, Weigand JE, Akabayov SR, Altincekic N, Bains JK, Banijamali E, Binas O, Castillo-Martinez J, Cetiner E, Ceylan B, Chiu LY, Davila-Calderon J, Dhamotharan K, Duchardt-Ferner E, Ferner J, Frydman L, Fürtig B, Gallego J, Grün JT, Hacker C, Haddad C, Hähnke M, Hengesbach M, Hiller F, Hohmann KF, Hymon D, de Jesus V, Jonker H, Keller H, Knezic B, Landgraf T, Löhr F, Luo L, Mertinkus KR, Muhs C, Novakovic M, Oxenfarth A, Palomino-Schätzlein M, Petzold K, **Peter SA**, Pyper DJ, Qureshi NS, Riad M, Richter C, Saxena K, Schamber T, Scherf T, Schlagnitweit J, Schlundt A, Schnieders R, Schwalbe H, Simba-Lahuasi A, Sreeramulu S, Stirnal E, Sudakov A, Tants JN, Tolbert BS, Vögele J, Weiß L, Wirmer-Bartoschek J, Wirtz Martin MA, Wöhnert J, Zetzsche H (2020). Secondary structure determination of conserved SARS-CoV-2 RNA elements by NMR spectroscopy. Nucleic Acids Res 48, 12415-12435.

3. Schnieders R[#], **Peter SA**[#], Banijamali E, Riad M, Altincekic N, Bains JK, Ceylan B, Fürtig B, Grün JT, Hengesbach M, Hohmann KF, Hymon D, Knezic B, Oxenfarth A, Petzold K, Qureshi NS, Richter C, Schlagnitweit J, Schlundt A, Schwalbe H, Stirnal E, Sudakov A, Vögele J, Wacker A, Weigand JE, Wirmer-Bartoschek J, Wöhnert J (2021). ^{1}H, ^{13}C, ^{15}N chemical shift assignment of the stem-loop 5a from the 5'UTR of SARS-CoV-2. Biomol NMR Assign 23, 1-9.

= shared first

4. **Peter SA**, Isaac JS, Narberhaus F, Weigand JE (2021). A novel, universally active C-terminal protein degradation signal generated by alternative splicing. JMB 433, Issue 8, 166890

5. Vögele J, Ferner J-P, Altincekic N, Bains JK, Ceylan B, Fürtig B, Grün JT, Hengesbach M, Hohmann KF, Hymon D, Knezic B, Löhr F, **Peter SA**, Pyper D, Qureshi NS, Richter C, Schlundt A, Schwalbe H, Stirnal E, Sudakov A, Wacker A, Weigand JE, Wirmer-Bartoschek J, Wöhnert J, Durchardt-Ferner E (2021). ^{1}H, ^{13}C,

^{15}N chemical shift assignment of the stem-loop 4 from the 5'UTR of SARS-CoV-2. Biomol NMR Assign 29, 1-6.

6. Sreeramulu S, Richter C, Berg H, Wirtz Martin MA, Ceylan B, Matzel T, Adam J, Altincekic N, Azzaoui K, Kaur Bains J, Blommers JJM, Ferner J, Fürtig B, Göbel M, Grün TJ, Hengesbach H, Hohmann KF, Hymon D, Knezic B, Martins J, Mertinkus K, Niestruk A, **Peter SA**, Pyper DJ, Qureshi NS, Scheffer U, Schlundt A, Schnieders R, Stirnal E, Sudakov A, Tröster A, Vögele J, Wacker A, Weigand JE, Wirmer-Bartoschek J, Wöhnert J, Schwalbe H (2021). Exploring the druggability of conserved RNA regulatory elements in the SARS-CoV-2 genome. Angew Chem Int Ed Engl 23.06.2021, doi: 10.1002/anie.202103693.

Statement of the contributions of SA Peter:

Nr. 1: 20% of the experiments, 10% writing

- Synthesis of the following vectors:
  - pETTrx1a_RRM1, pETTrx1a_RRM2, pETTrx1a_RRM1+2, pDLP_UCP3_mut5_NMR
- Synthesis of the following RNA samples:
  - CDE1, CDE1_GG, CDE2, CDE2_GG, CDE1-2
- Performance of Luciferase assays
- Manuscript writing

Nr. 2/3/5/6: 13/10/8/8% of the experiments, 5/35/0/0% writing

- Synthesis of the following vectors:
  - pHDV_3_s2m, pHDV_3_SL1, pHDV_3_SL2, pHDV_3_SLbase, pHDV_5_SL1, pHDV_5_SL1-4, pHDV_5_SL1-4, pHDV_5_SL2+3, pHDV_5_SL4, pHDV_5_SL4sh, pHDV_5_SL5a, pHDV_5_SL5b+c, pHDV_5_SL5 stem, pHDV_5_SL6, pHDV_5_SL7, pHDV_5_SL8, pHDV_5_SL8 loop, pHDV_att_hairpin, pHDV_pseudoknot, pHDV_pseudoknot short, pSP64_HDV_3_SL3_base, pSP64_HDV_3_SL1, pSP64_HDV_3' UTR, pSP64_HDV_5' UTR and pSP64_HVR.
- Generation of DNA template for *in vitro* transcription:
  - pHDV_5_SL5B+C, pHDV_5_SL5a, pHDV_3_SL2, pHDV_5_SL1 and pHDV_3_SL3stem
- Manuscript writing

Nr. 4: 90% of the experiments, 90% writing

- SA Peter: construct synthesis and Western blots for Figure 1B, C, and D, Figure 2, Figure 3 as well as Supplementary Figures 3, 5, 6, 7, 8
- SA Peter: manuscript writing
- JS Isaac: construct synthesis and Western blots for Supplementary Figures 1a, 2 and 4, RT-PCRs in Figure 1
- JE Weigand: manuscript writing
- F Narberhaus: advice for *E. coli* experiments

11. Curiculum Vitae

Personal Information

Name: Stephen A. Peter
Date of birth: 03.08.1989 (Offenbach a.M.)

Education

01/2017 – 12/2021 Doctoral candidate
Working Group Weigand
Technische Universität, Darmstadt

07/2015 – 03/2016 Master thesis
Prof. Dr. Dorothea Schulte, Edinger-Institute Frankfurt a.M.
“Untersuchungen des Chromatinzustandes während der Differenzierung von ESCs zu NPCs“

10/2013 – 03/2016 Master student
Degree: Master of Science in technical biology
Technische Universität, Darmstadt

07/2013 – 10/2013 Bachelor thesis
Prof. Dr. Bodo Laube, Technische Universität Darmstadt
„Glutamatrezeptoren in neuronalen Stammzellen“

10/2010 – 10/2013 Bachelor student
Degree: Bachelor of Science in biology
Technische Universität, Darmstadt

09/2006 – 06/2009 upper secondary school
Claus-von-Stauffenberg-Schule
Rodgau-Dudenhofen, Hessen

Experience

09/2014 – 01/2017 Scientific assistance for
Dr. med. Klaus Peter at Frankfurt a. M.

12. Ehrenwörtliche Erklärung

Ich erkläre hiermit ehrenwörtlich, dass ich die vorliegende Arbeit entsprechend den Regeln guter wissenschaftlicher Praxis selbstständig und ohne unzulässige Hilfe Dritter angefertigt habe.
Sämtliche aus fremden Quellen direkt oder indirekt übernommenen Gedanken sowie sämtliche von Anderen direkt oder indirekt übernommenen Daten, Techniken und Materialien sind als solche kenntlich gemacht. Die Arbeit wurde bisher bei keiner anderen Hochschule zu Prüfungszwecken eingereicht. Die eingereichte elektronische Version stimmt mit der schriftlichen Version überein.

Darmstadt, den 28.02.2022

_____

Stephen Peter